

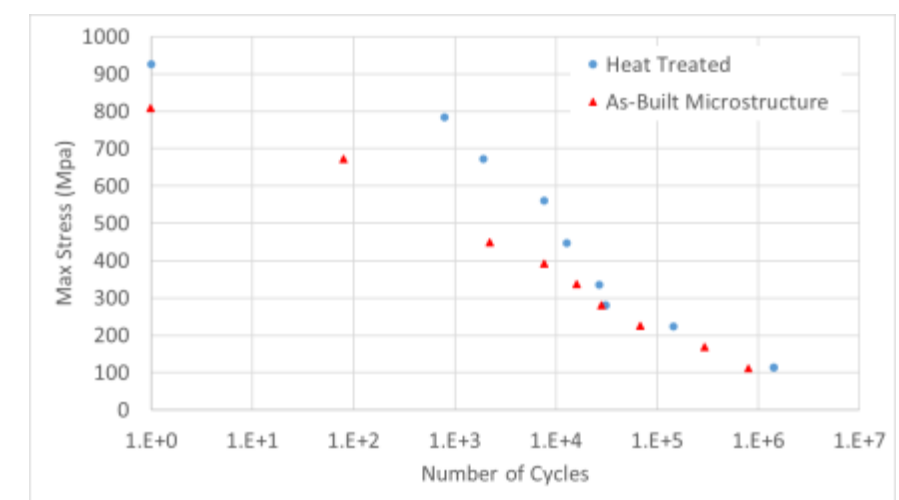
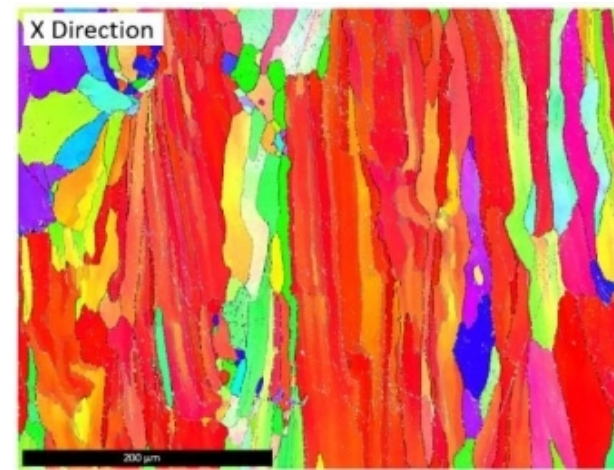
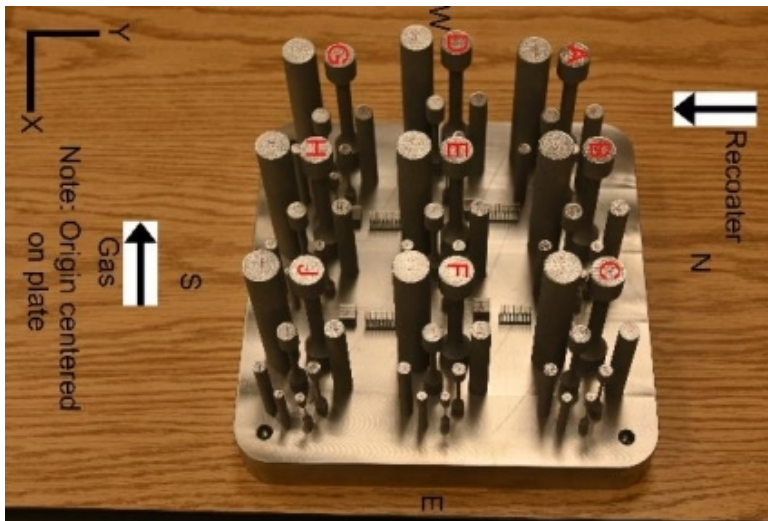
Fatigue Behavior Of Additively Manufactured Ti-5553 (and Ti-6Al- 4V)

**Jay D. Carroll, Zachary Casias, Christopher Laursen, Philip
Noell, John Emery**

Sandia National Laboratories, Albuquerque, NM

Research Questions:

1. How does heat treatment affect AM Ti-5553 fatigue properties?
 - β vs α - β
2. Are AM Ti-6Al-4V fatigue lives size-dependent?
3. How do properties compare to literature?
 - More flaws in AM vs conventional processing
 - Effects of surface roughness



Ti-5553 vs Ti-6Al-4V



- **Ti-5553 near beta alloy**
 - 5% Al, 5% Mo, 5% V, 3% Cr, 0.5% Fe
 - Yield Strength \approx 900 MPa
 - Ultimate Strength \approx 1000 MPa
 - Some commercial use. Being explored as an AM alloy.
- **Ti-6Al-4V alpha-beta alloy**
 - 6% Al, 4% V
 - Yield Strength \approx 900 MPa
 - Ultimate Strength \approx 925 MPa
 - Widespread commercial use and most common AM Ti alloy.
- **Why use Ti-5553 for additive manufacturing?**
 - Lower elastic modulus in the beta (as-printed) condition.
 - Can resist hot cracking more than Ti-6Al-4V.
 - Can be heat treated to alpha-beta condition, high strength and good ductility

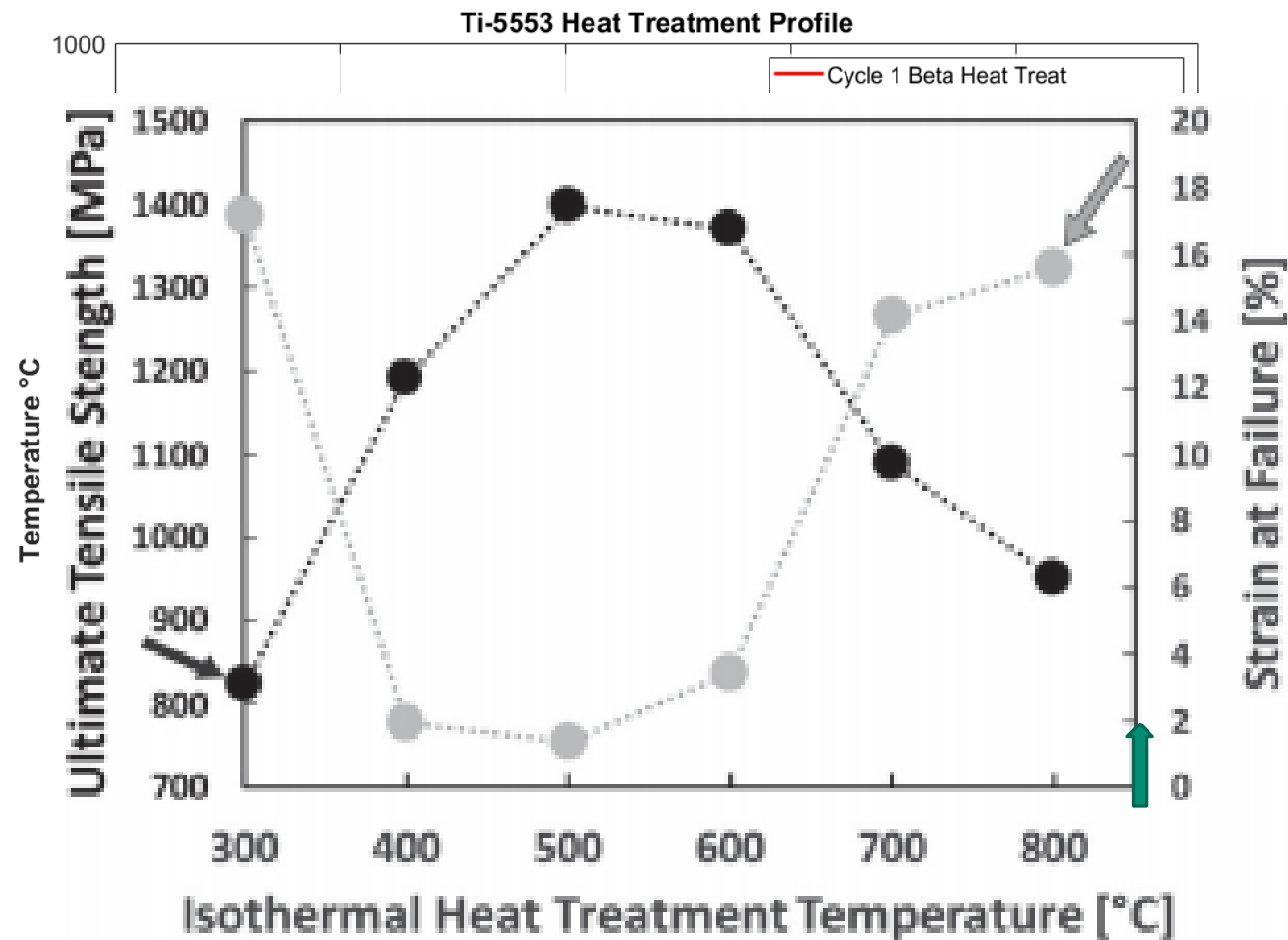
Ti-5553 Heat Treatment



- Elastic modulus can change by factor of 2 depending on α/β mixture!

Carlton *et al.*, *Sci. Technol. Weld. Join.* 24 (2019) 465-473

	Heat-treatment temperature (°C)	E (GPa)
Our as-built	300	$\sim 100\% \beta$
	400	66 ± 3
	500	98 ± 4
	600	97 ± 1
	700	92 ± 1
Our heat treated (900°C)	800	$25\% \alpha, 75\% \beta$
	900	$25\% \alpha, 75\% \beta$
		91



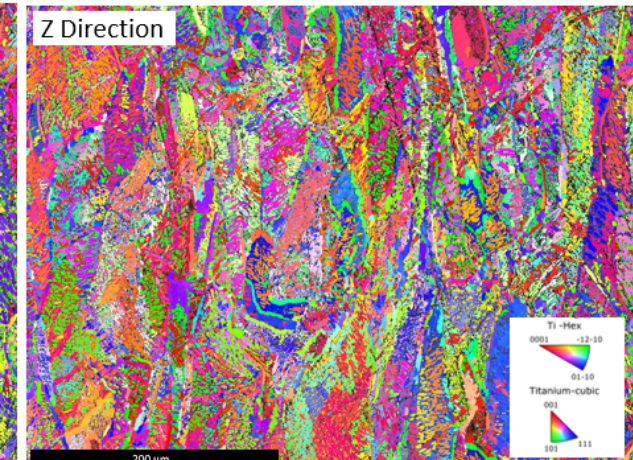
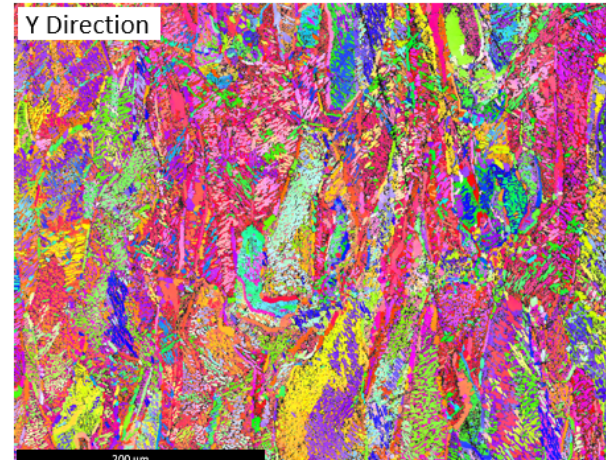
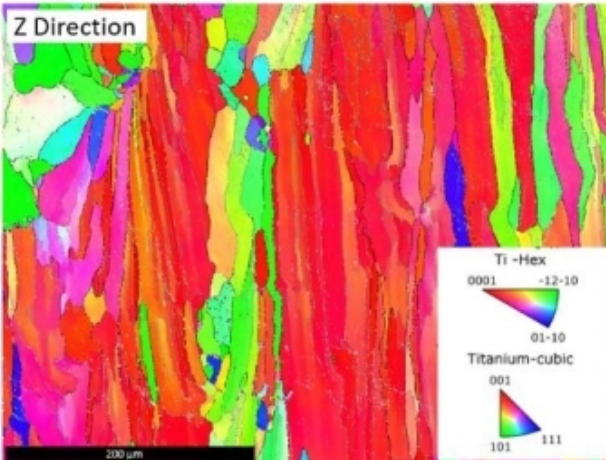
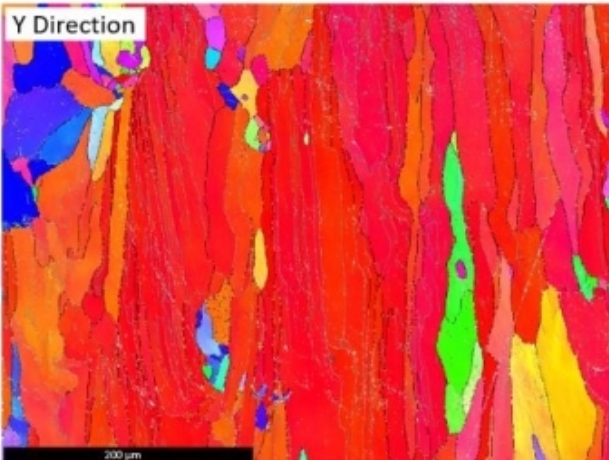
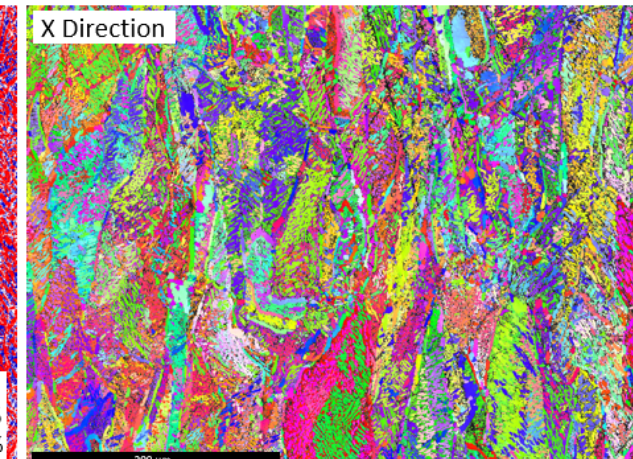
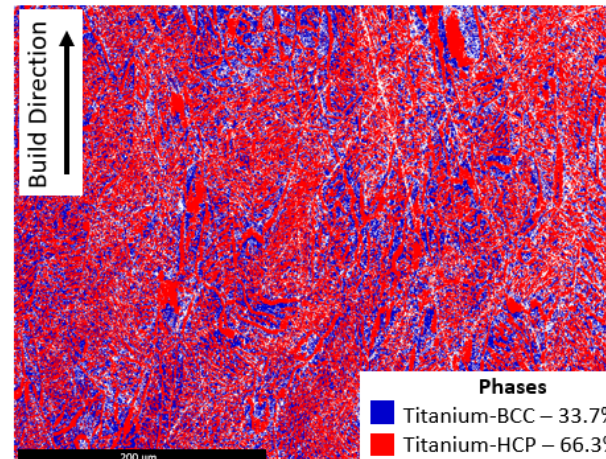
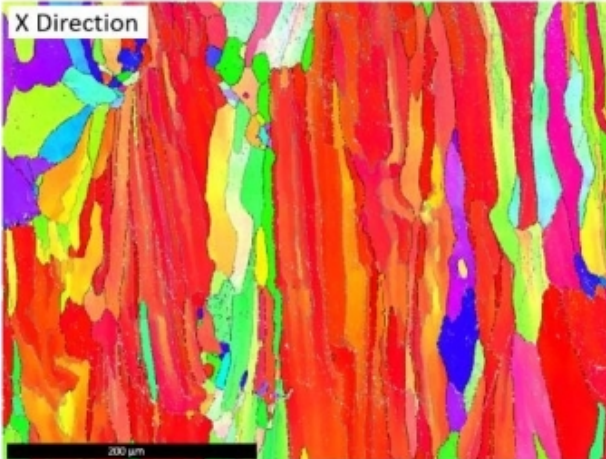
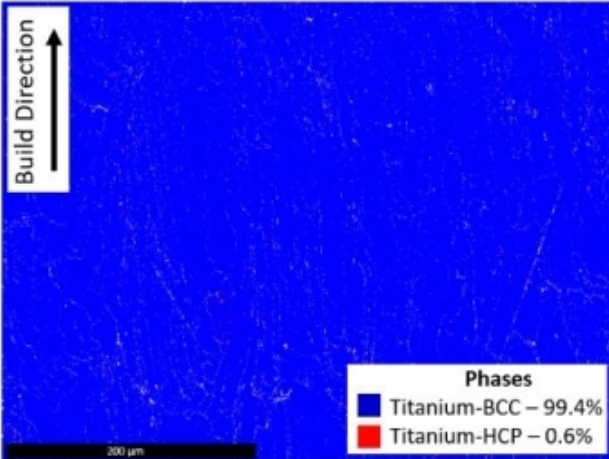
AM Ti-5553 Microstructure



α = HCP (red)

β = BCC (blue)

ω = Hexagonal (detrimental, not detected)



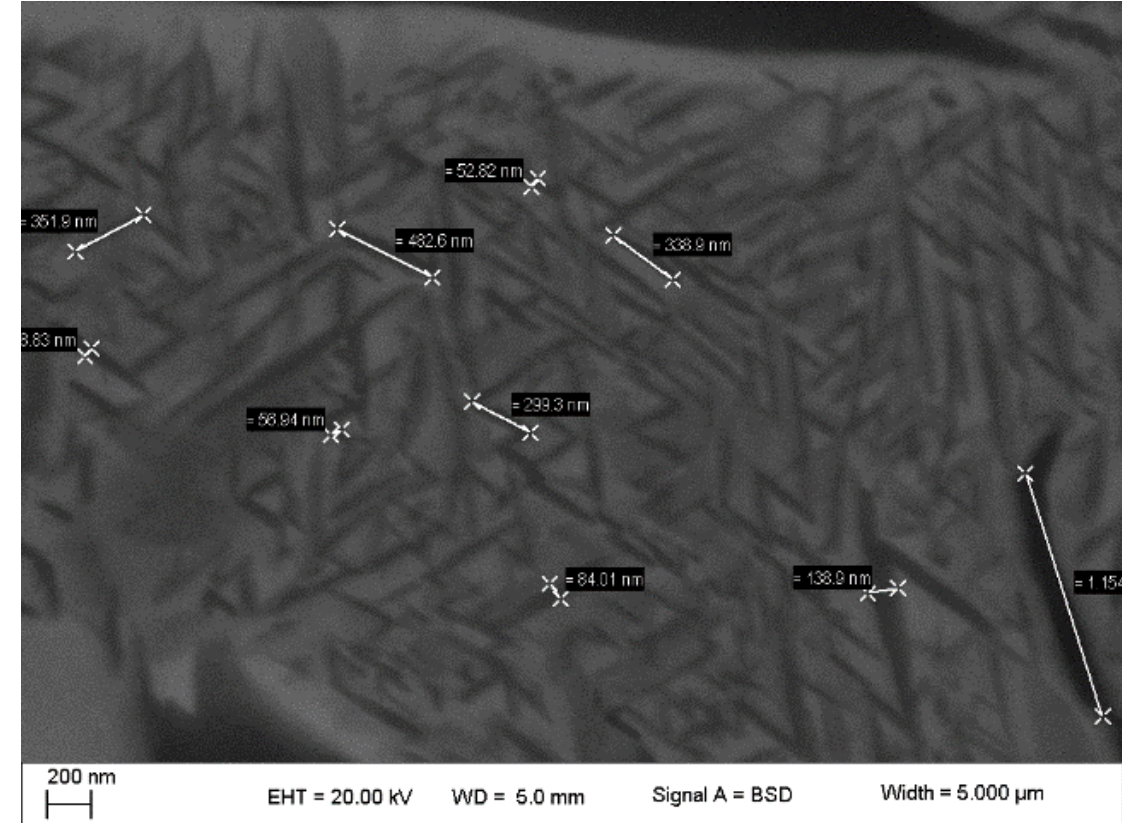
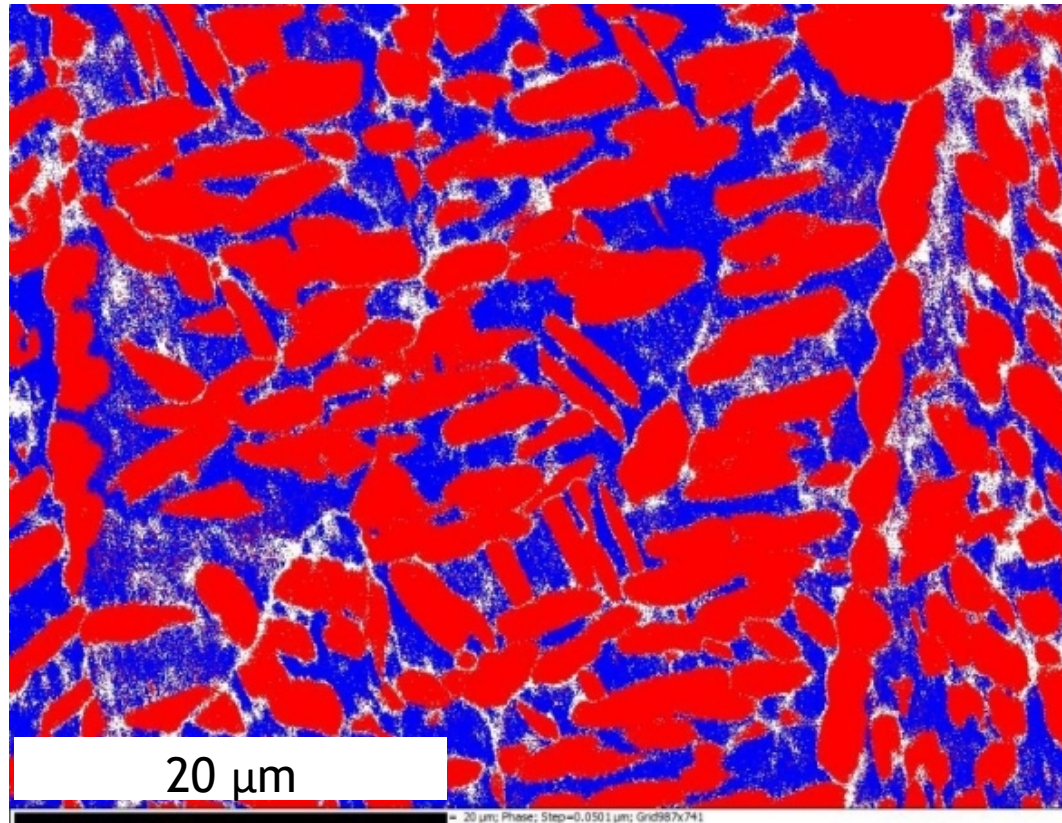
- As-printed has columnar microstructure, pure BCC with [100] in the build direction.
- Heat treated has 33% Beta and 67% alpha in laths at several size scales:
- $\sim 7 \times 1 \mu\text{m}$ and $\sim 300 \times 50 \text{ nm}$.

AM Ti-5553 Microstructure



α = HCP (red)
 β = BCC (blue)
 ω = Hexagonal (detrimental, not detected)

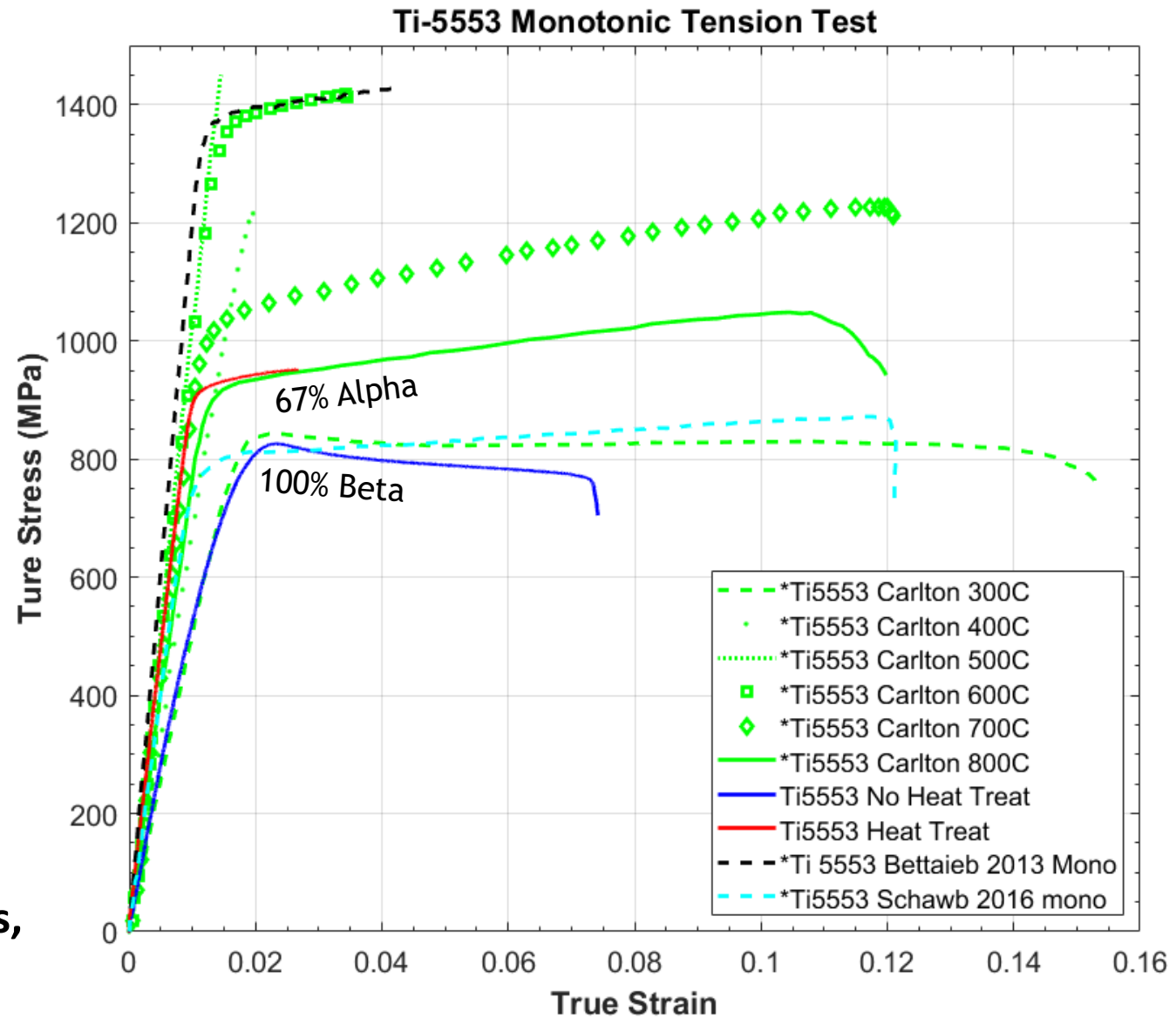
- Heat treated Ti-5553 has 33% β and 67% α in laths at several size scales:
- Fine α laths $\sim 7 \times 1 \mu\text{m}$
- Coarse α laths $\sim 300 \times 50 \text{ nm}$.



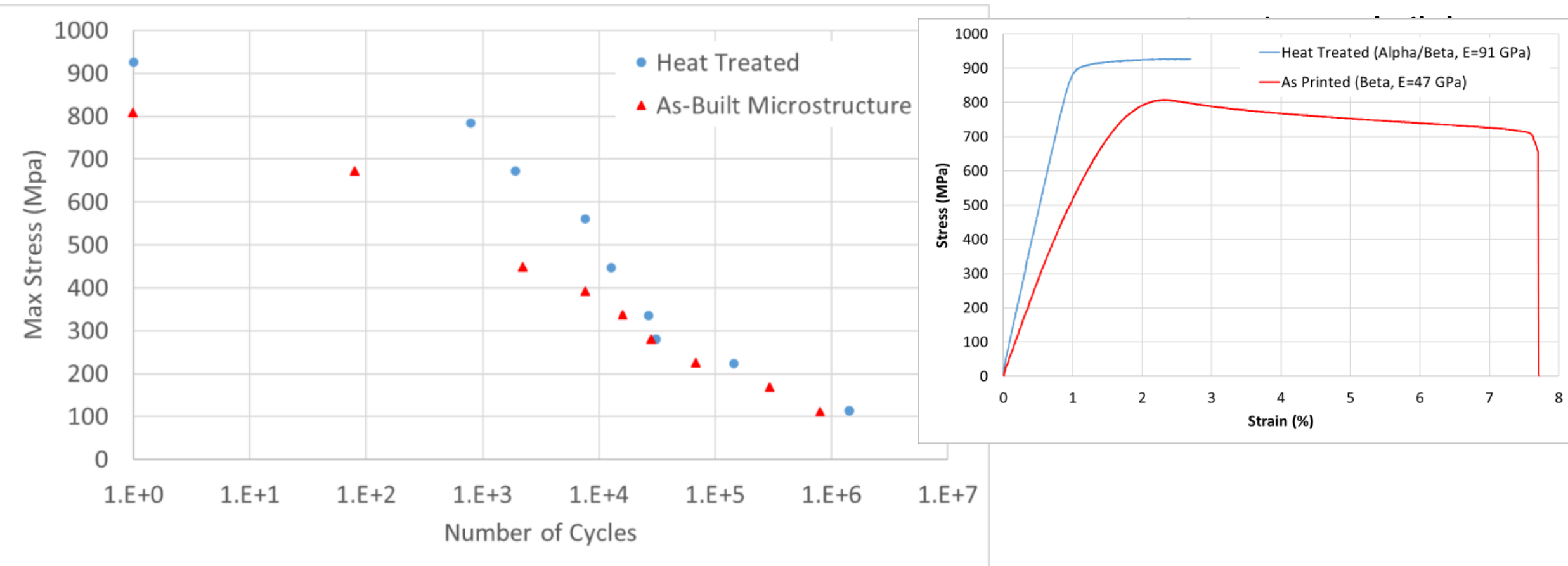
This AM Ti-5553 is inline with published values



- Strengths are in-line with published values, but ductilities are lower.

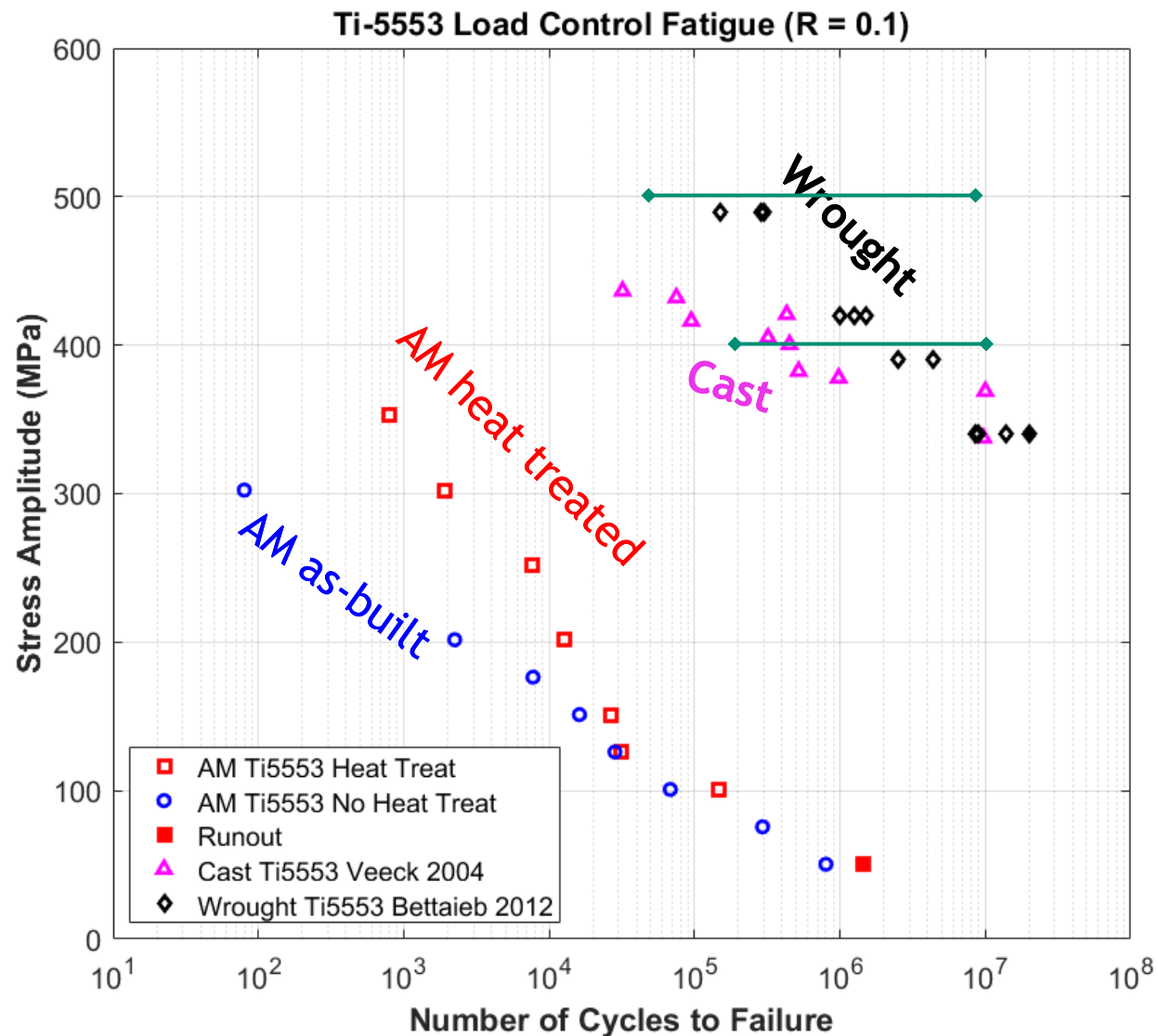


AM Ti-5553 Stress Life Fatigue Curves



- Steep drop-off in fatigue strengths with no clear threshold.
- Similar behavior in high cycle fatigue regime ($>10,000$ cycles).
- Heat-treated experiences more microplasticity in the LCF regime leading to shorter lifetimes.

This AM Ti-5553 has fatigue lives far below published values for wrought and cast Ti-5553.

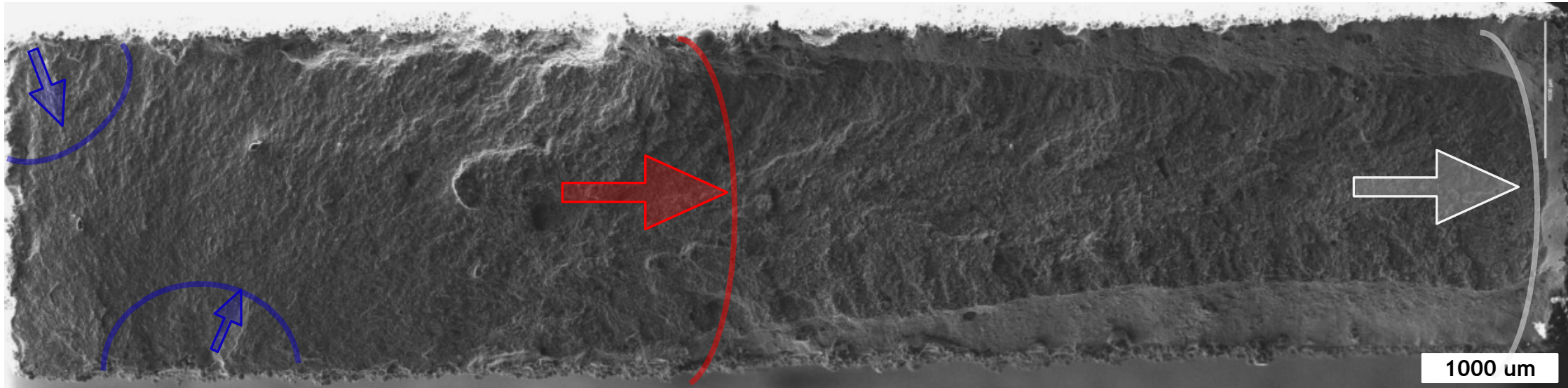


- This AM Ti-5553 has fatigue properties far below conventionally processed Ti-5553.
- Is it inherent to AM or just our AM.
- Yasin also tested AM Ti-5553 in fatigue, at $R=-1$, round, heat treat to 900C.

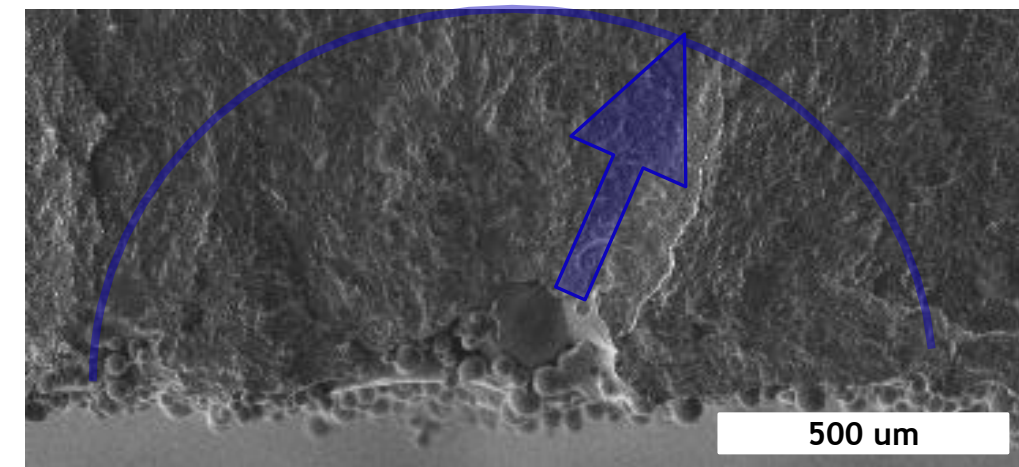
Possible causes:

- Coarse alpha from excessive heat treatment.
- Flaws from AM.
- Surface roughness and aspect ratio of sample.

AM Ti-5553 fatigue nucleates at near-surface voids



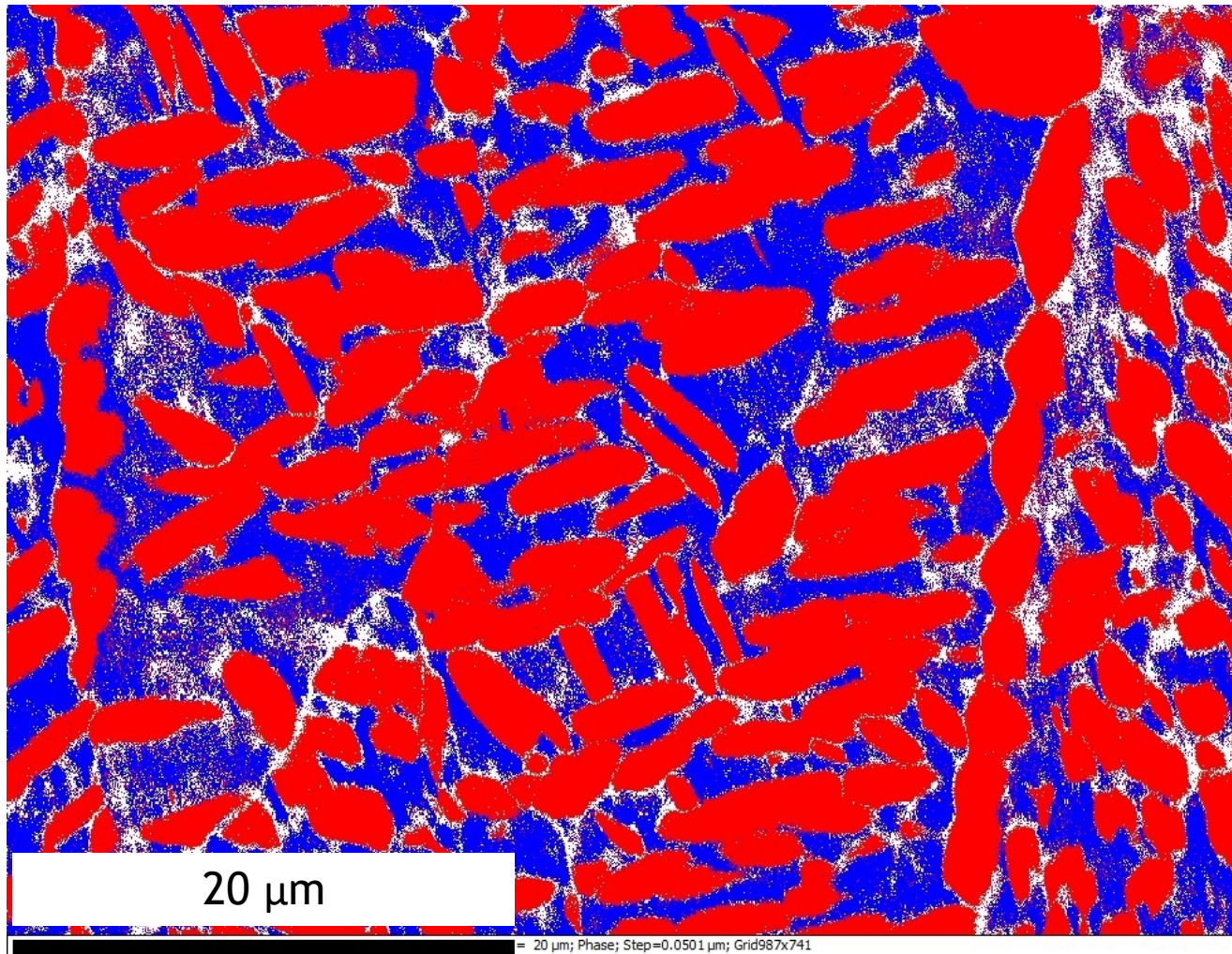
- Fracture surfaces show failure dominated by surface defects.
- Machining specimens could remove near-surface voids and lead to artificially high fatigue strengths.



Lower fatigue strength of AM Ti-5553

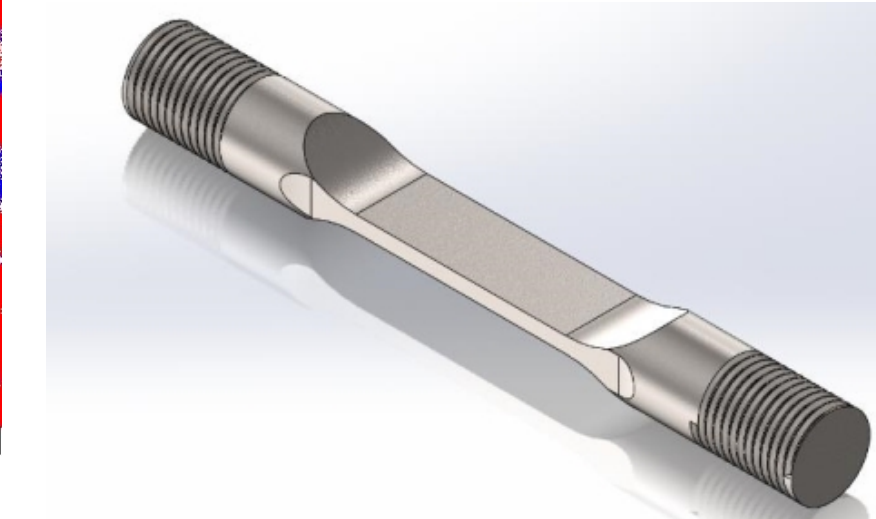
α = HCP (red)

β = BCC (blue)



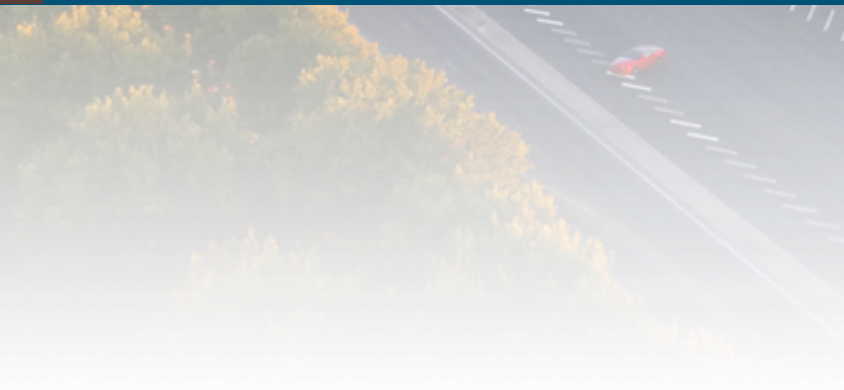
Possible causes:

- Coarse alpha from excessive heat treatment.
- Flaws from AM.
- Surface roughness and aspect ratio of sample.



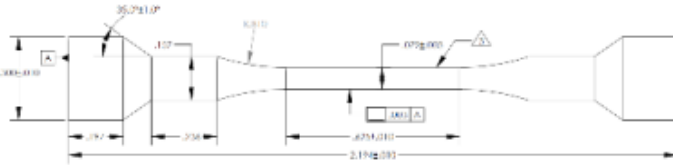


Ti-6Al-4V

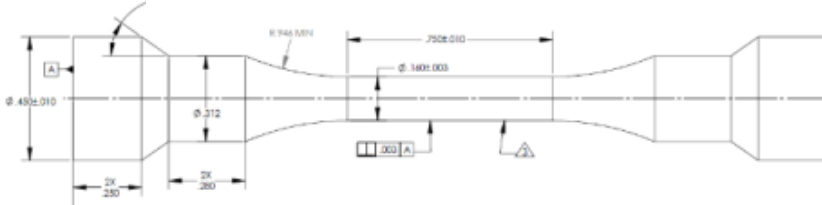


AM Ti-6Al-4V Tensile/fatigue samples

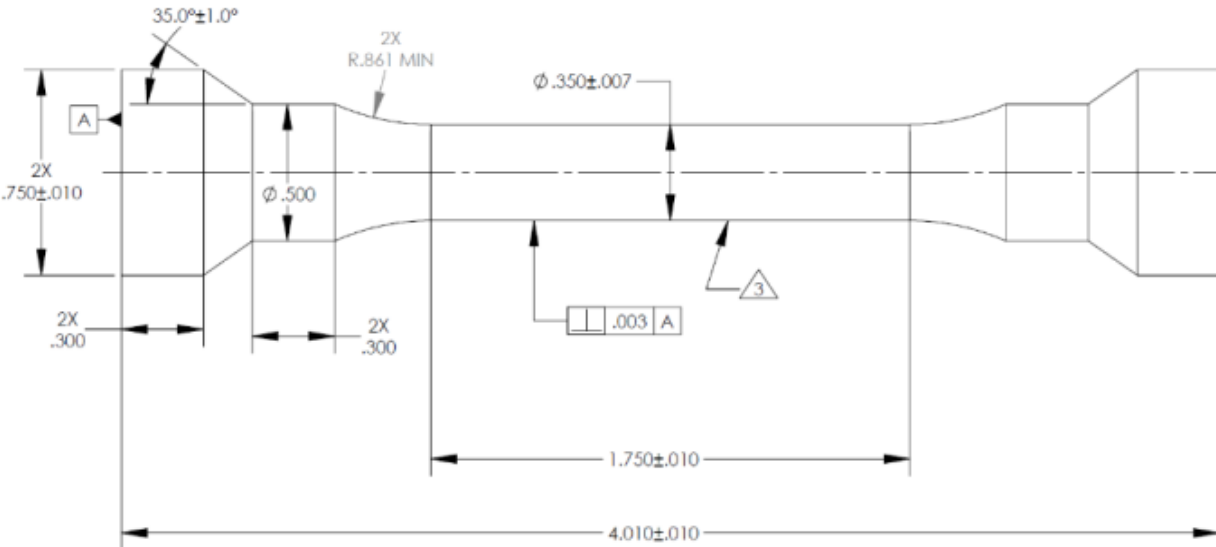
- Annealing heat treatment at 704°C for 2 hrs in vacuum $<10^{-5}$ torr. Cooling rates of 5°Cmin.



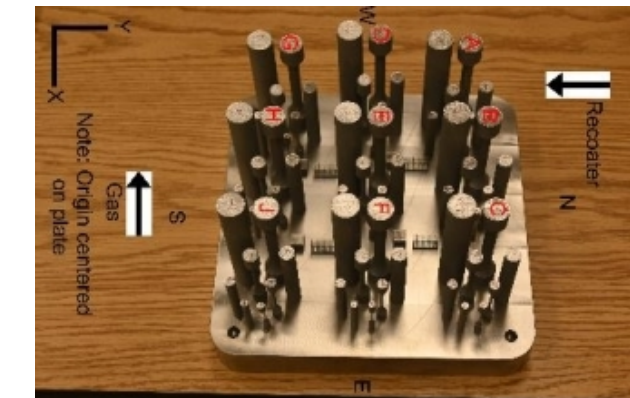
R6
15.9 mm long x 2mm dia



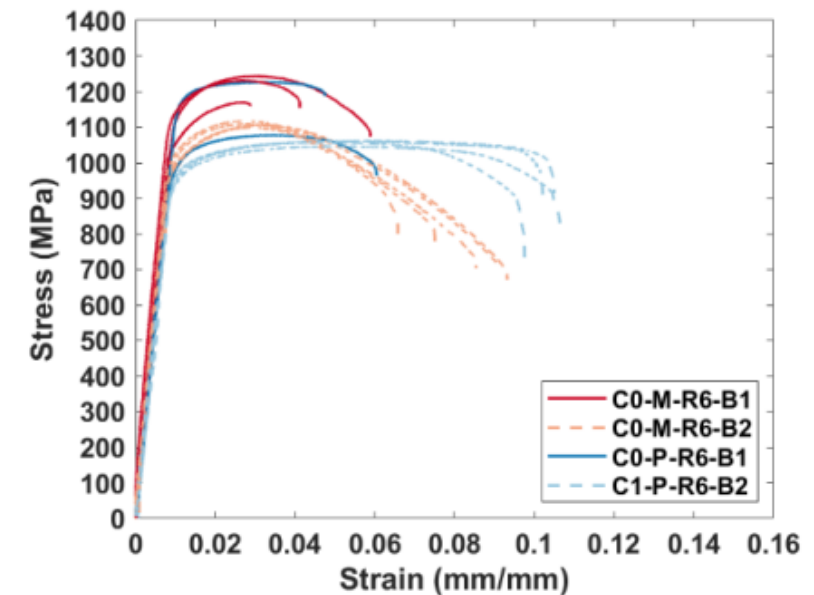
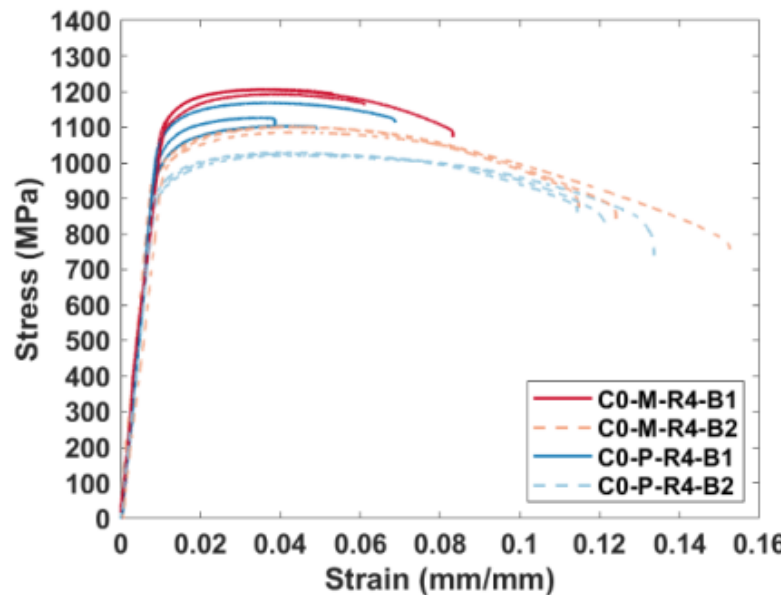
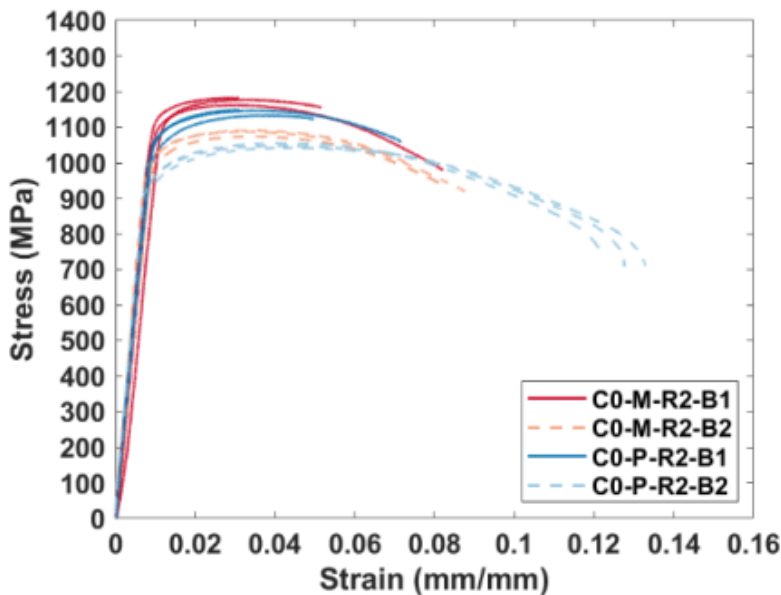
R4
19 mm long x 4.1 mm dia



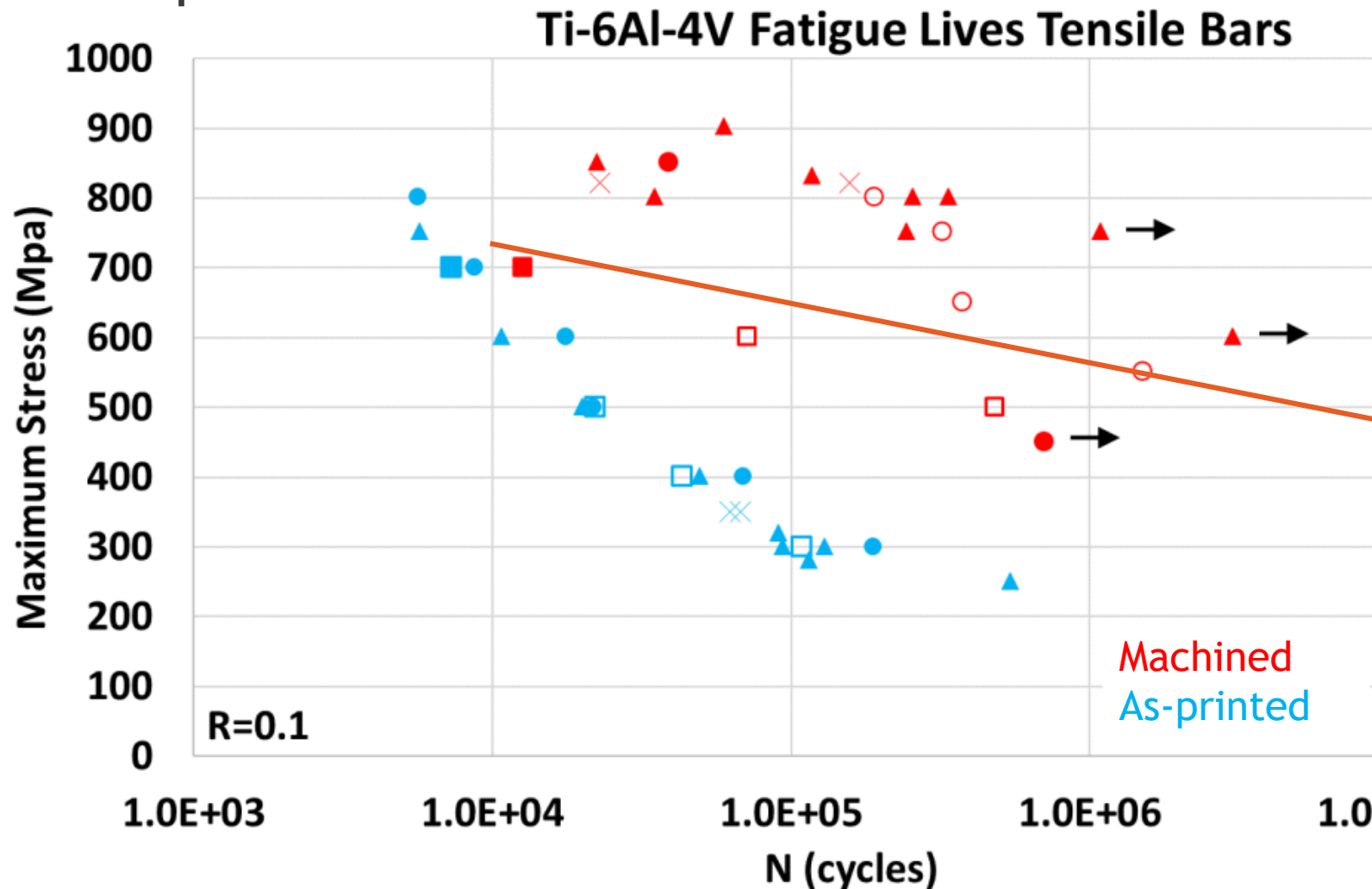
R2
45 mm long x 8.9 mm dia



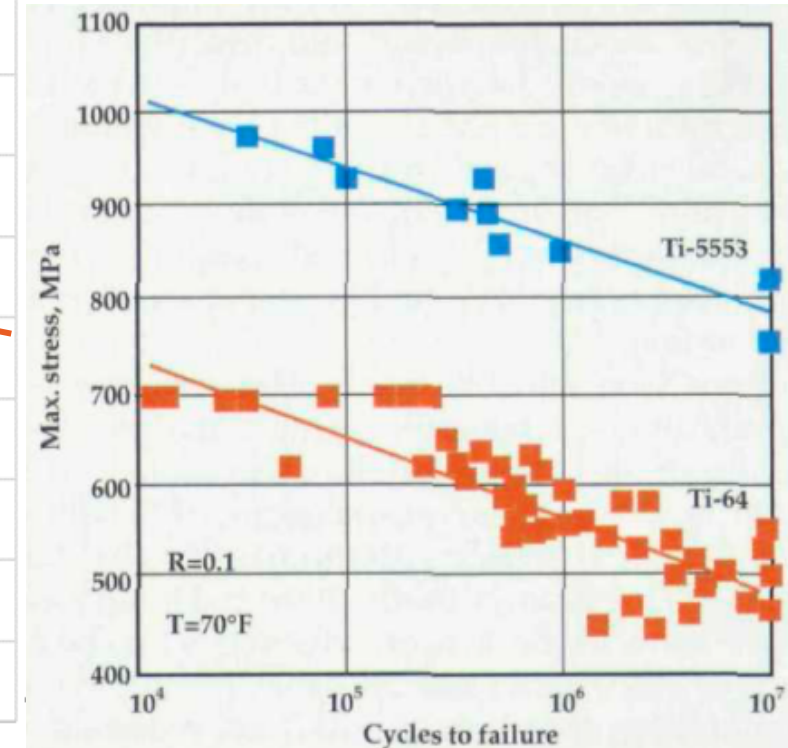
AM Ti-6Al-4V Tensile Results



AM Ti-6Al-4V fatigue lives appears to be size-independent

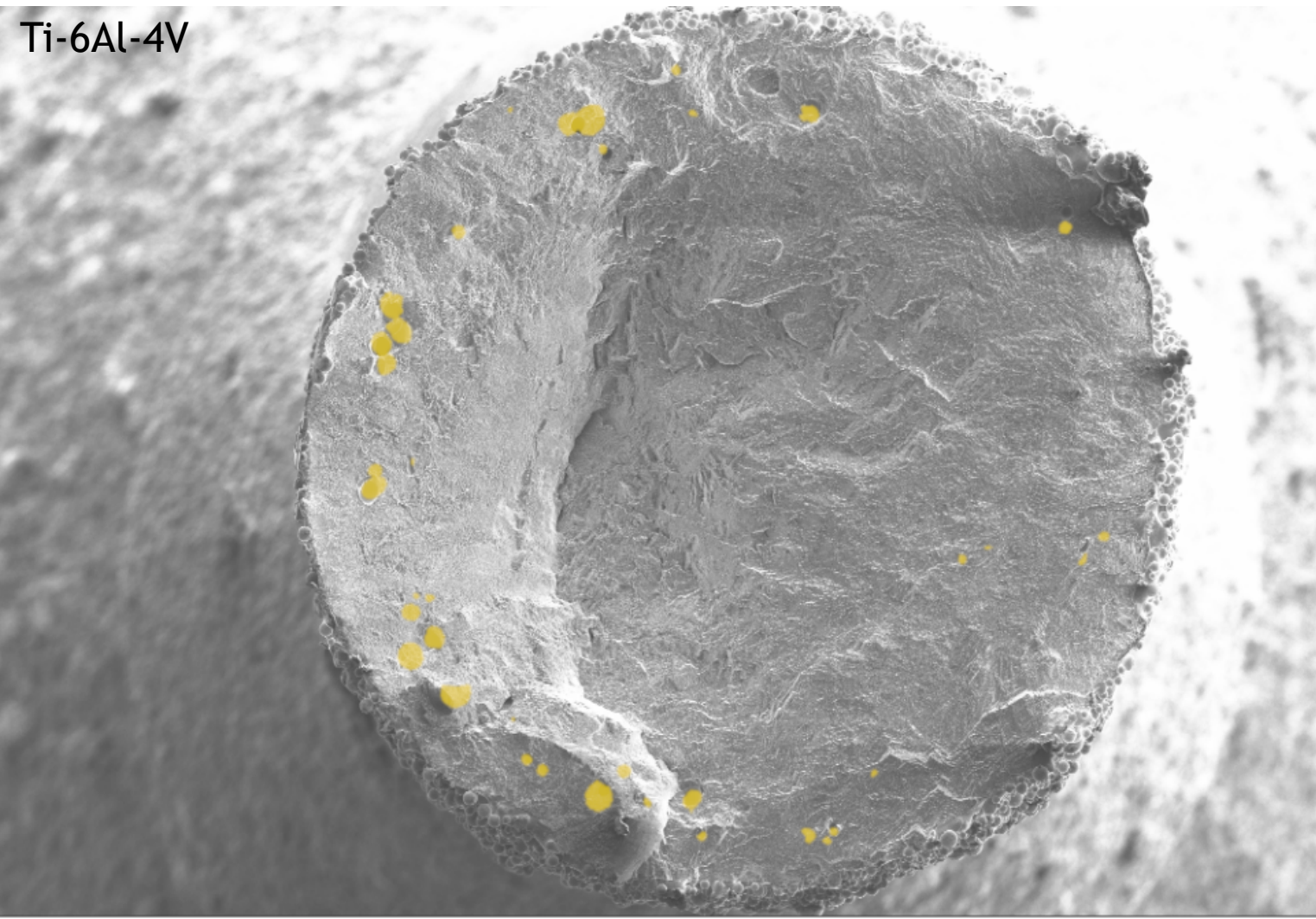


Veeck et al., J. Advanced Mat, 2005
Cast and machined



- Machined specimens outperform AM surfaces.
- Specimens with AM surfaces are much more predictable.
- No measurable size effects between as-printed R2, R4, R6 samples

AM Ti-6Al-4V size independence may be related to voids at the contour-fill interface



- **Machined specimens significantly outperform as-printed specimens, but with more noise.**
 - **Enough voids in as-printed to make lives deterministic?**
- **Voids near surfaces due to interface between contour pass and fill hatch.**

Conclusions

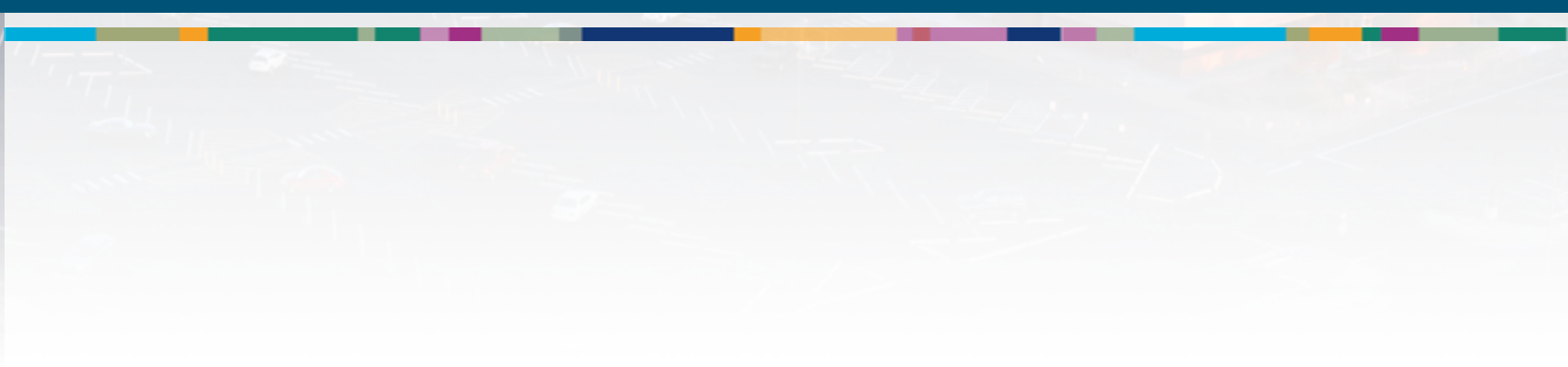


- Some of the first measurements of fatigue of AM Ti-5553.
- Pure beta vs 75% alpha 25% beta alloys exhibited equivalent fatigue lives in high cycle fatigue.
 - In low cycle fatigue, alpha/beta appears to outperform pure beta.
- Ti-6Al-4V fatigue lives were independent of specimen size
 - Increasing void probability with increasing size balances with increased surface crust with decreasing size.

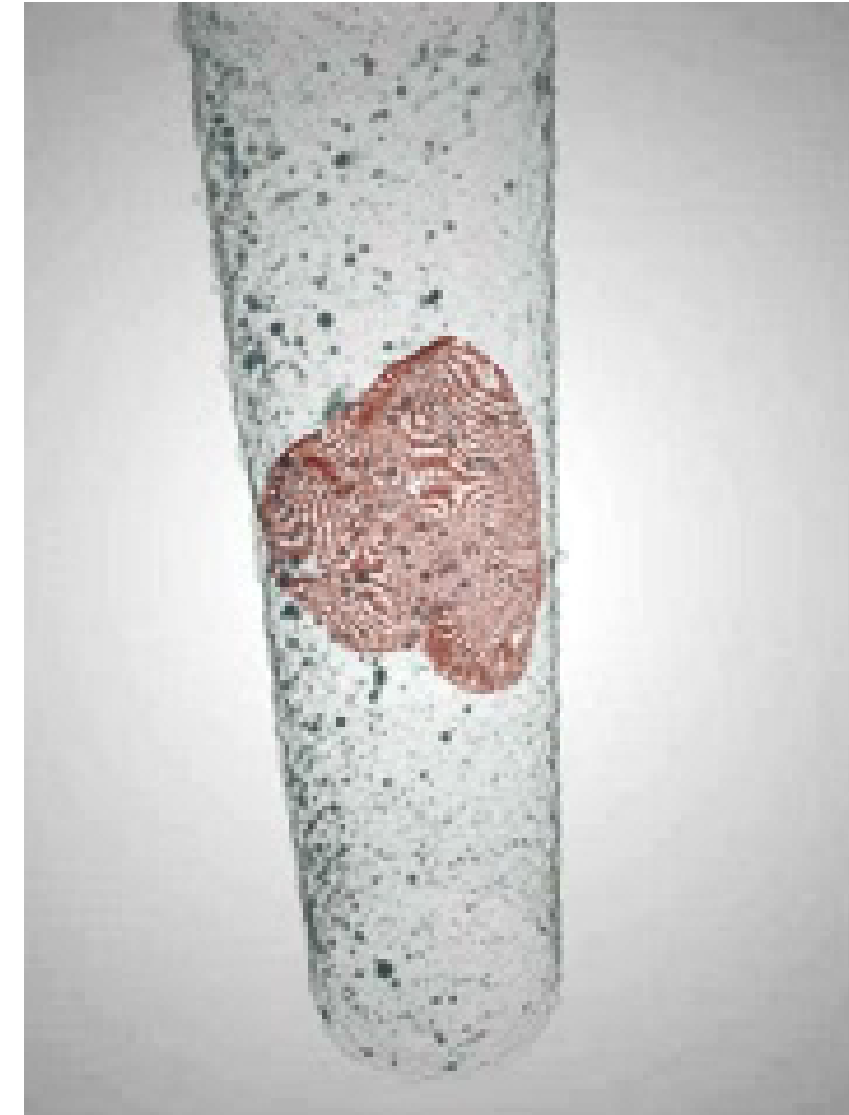
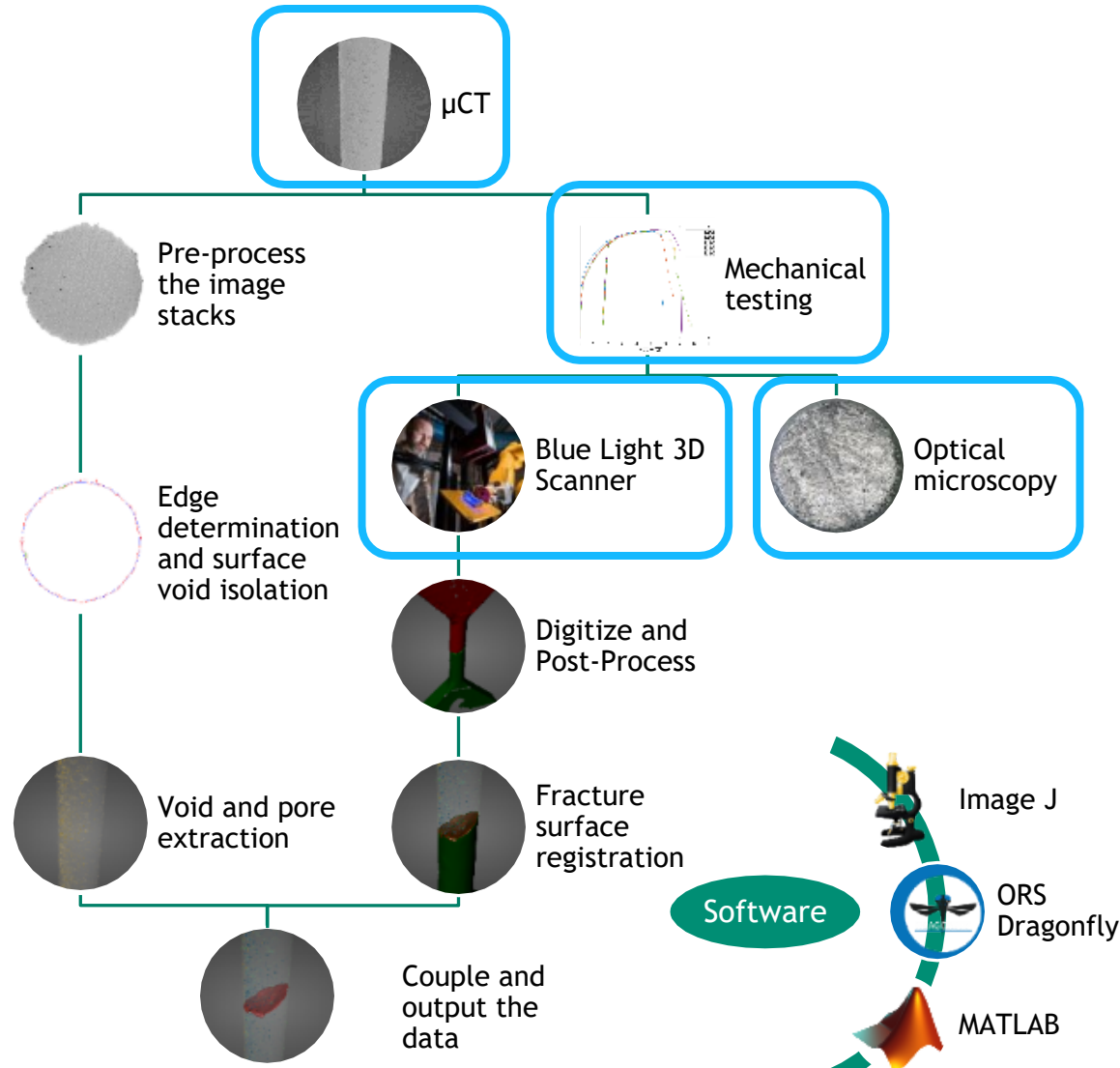


Future work: can we attribute failure location to specific defects?

Heat treated AlSi10Mg, tension

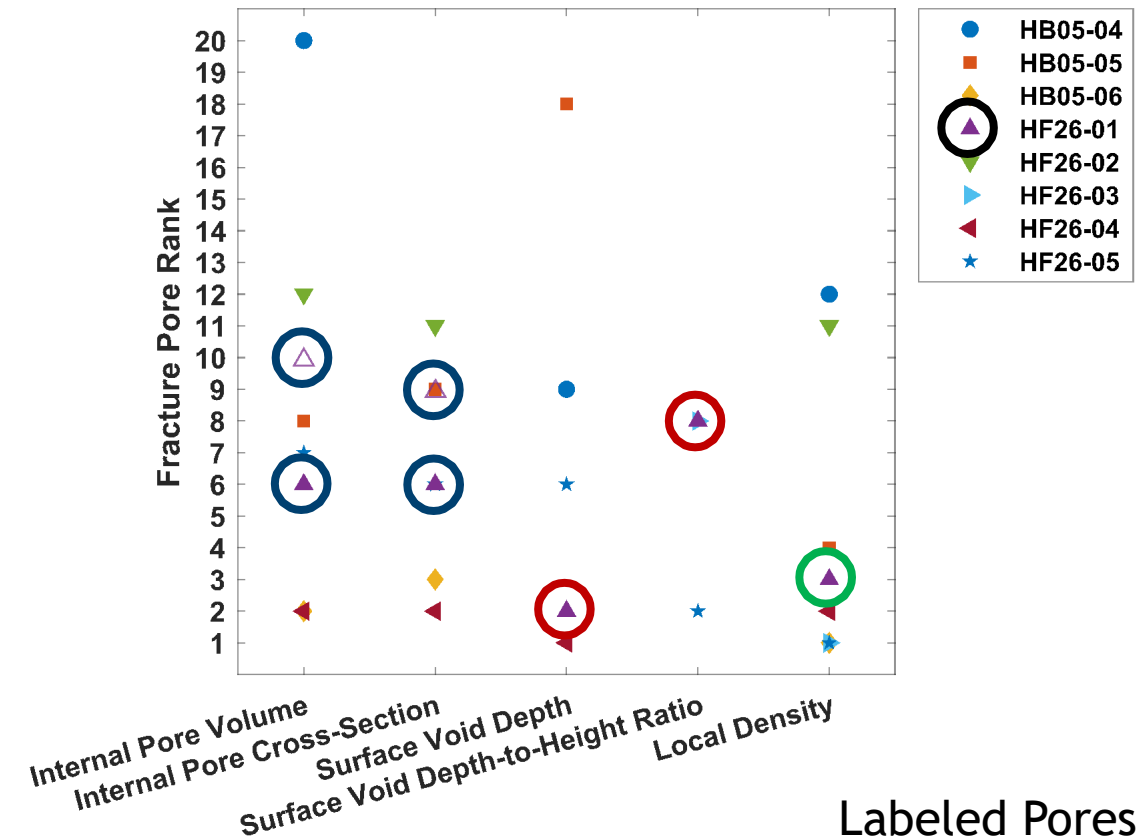
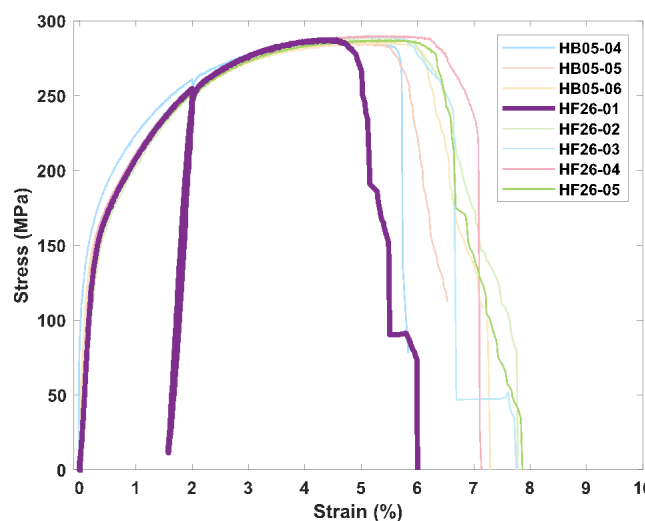
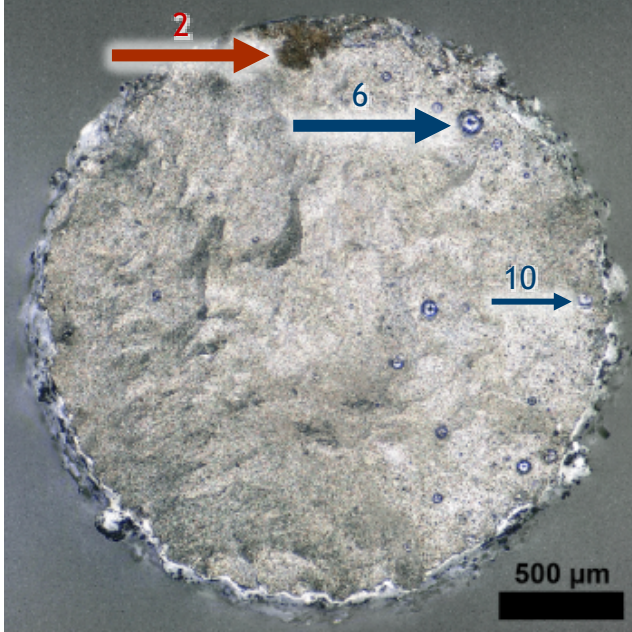


Ex-situ Correlation of Computed Tomography and Fracture Location



C.M. Laursen, P.J. Noell, J.D. Carroll, "Ex-situ Correlation of Fracture Location to Internal Defects in AM AlSi10Mg via micro Computed Tomography", *In Preparation*

Failure of specimen HF26-01 was largely determined by surface void depth.



HF26-05	Internal Pore Volume	Internal Pore Cross-Section	Surface Void Depth	Surface Void Depth-to-Height	Local Density
Rank	6	6	2	8	3
Pore Label	83322	83322	83964	7520	1297
Fracture Value	730,294 μm^3	10,522 μm^2	168.8 μm	9.49	99.727 %
Peak Value	2,045,810 μm^3	24,204 μm^2	197.1 μm	16.67	99.687 %

Acknowledgements



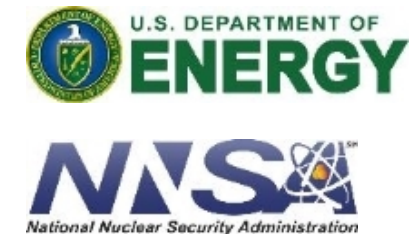
Sandia National Laboratories

Dale Cillessen, Jessica Buckner

National Security Campus

Ben Brown, Andy Deal

Authors: Jay D. Carroll, Zachary Casias, Christopher Laursen, Philip Noell, John Emery

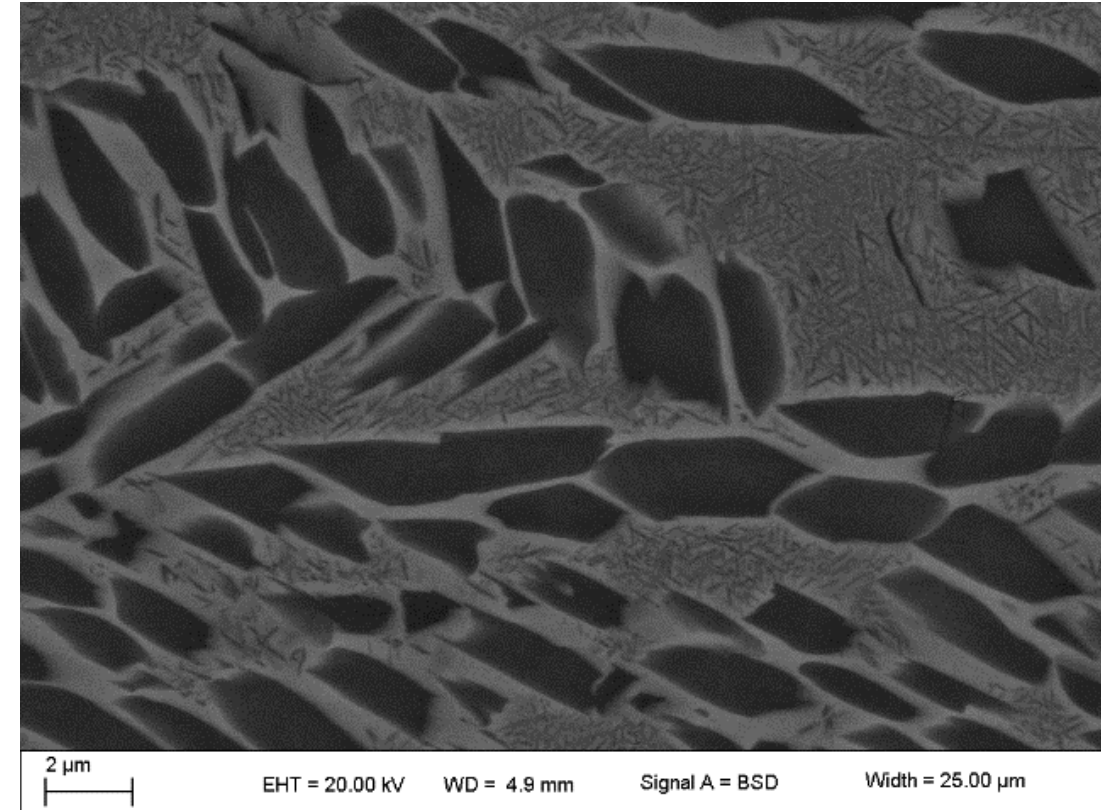
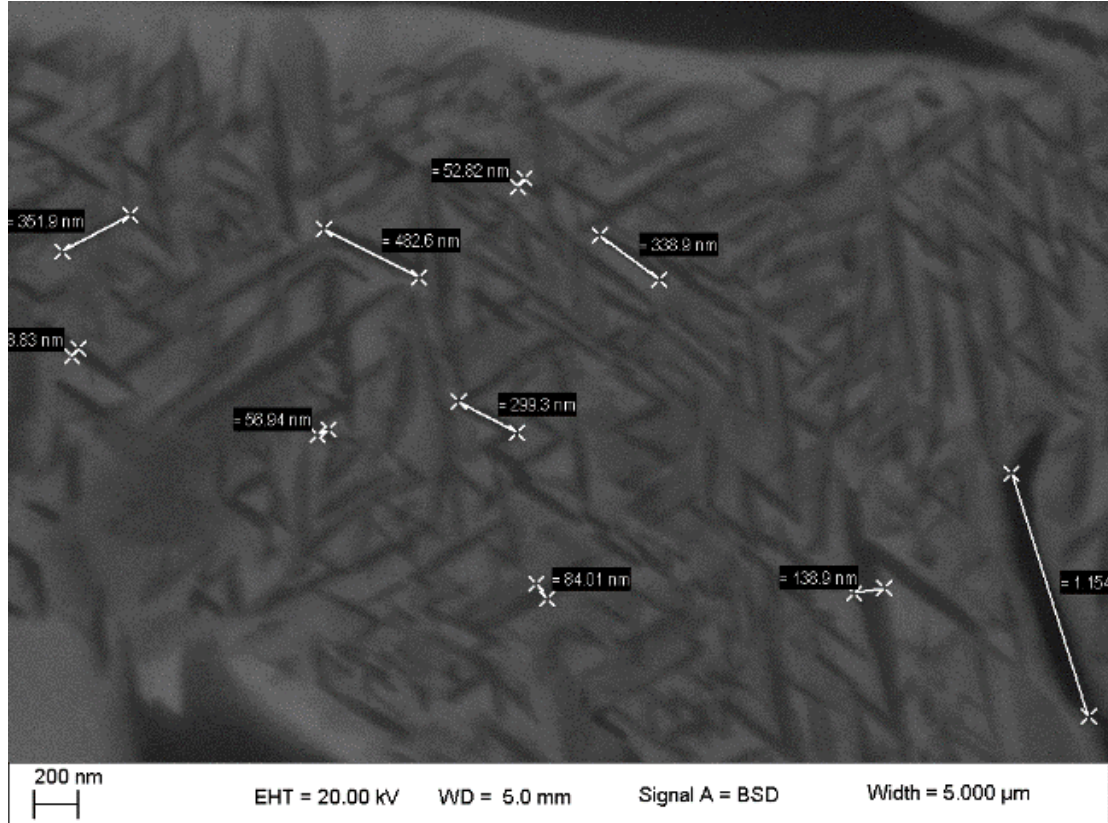




Extra Slides



High resolution images of alpha laths in AM Ti-5553





CT relate voids to fracture?

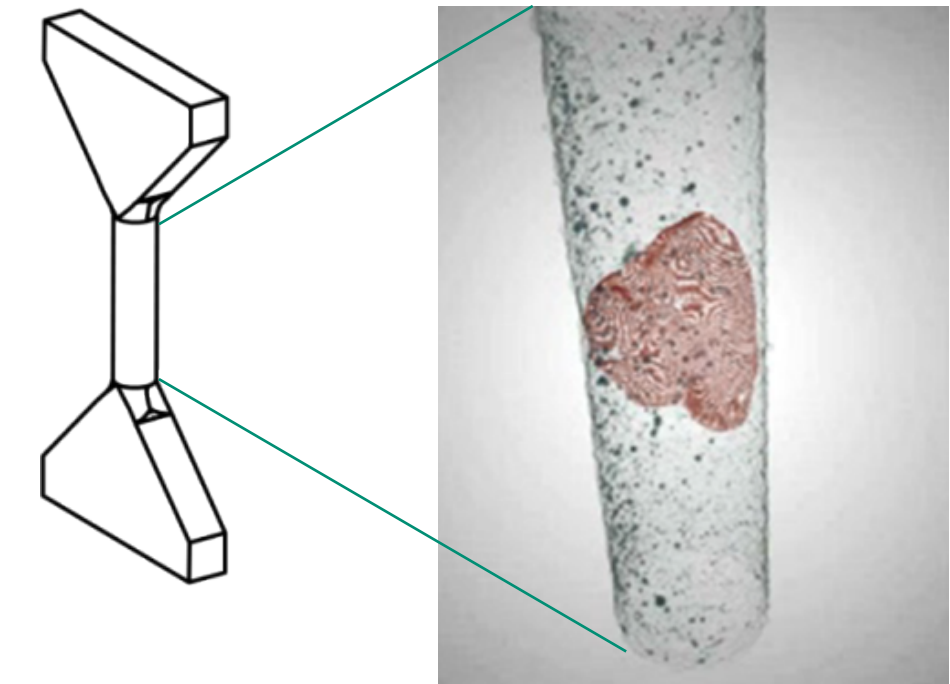
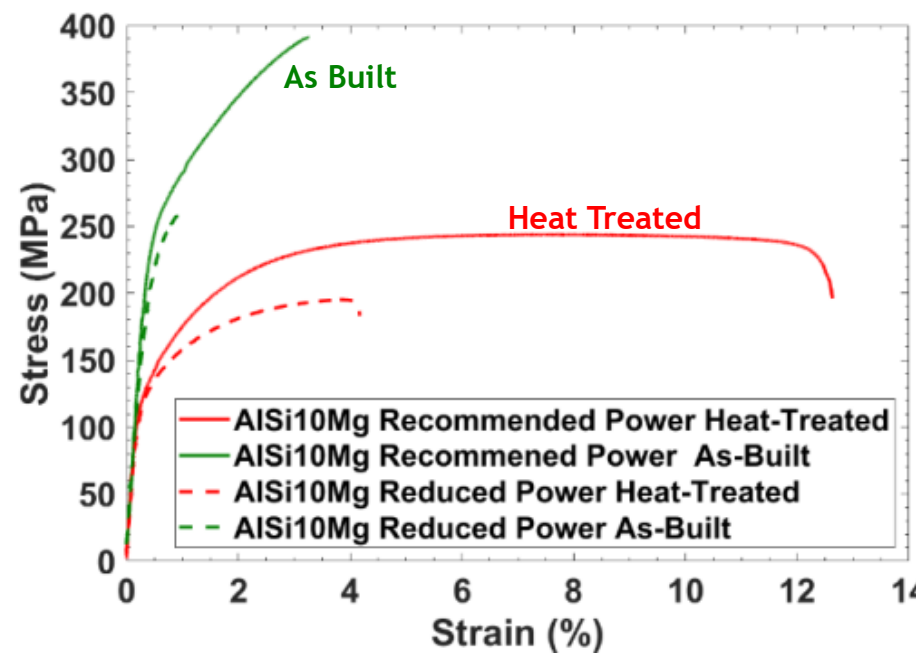
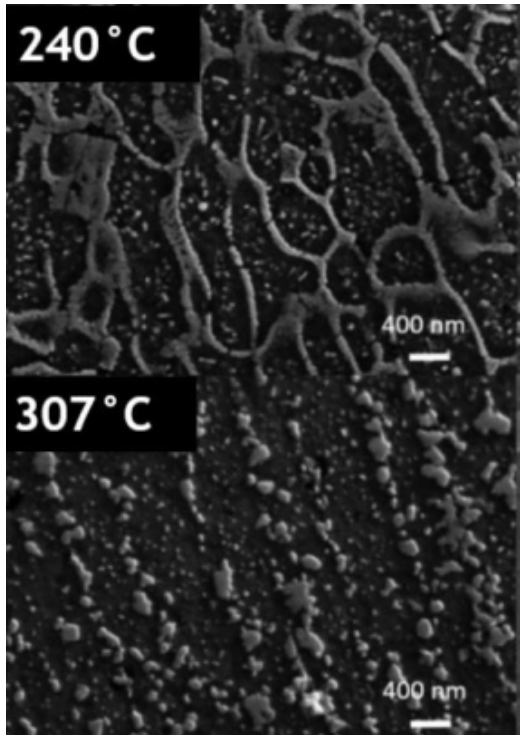
Heat treated AlSi10Mg, tension



Research Questions:

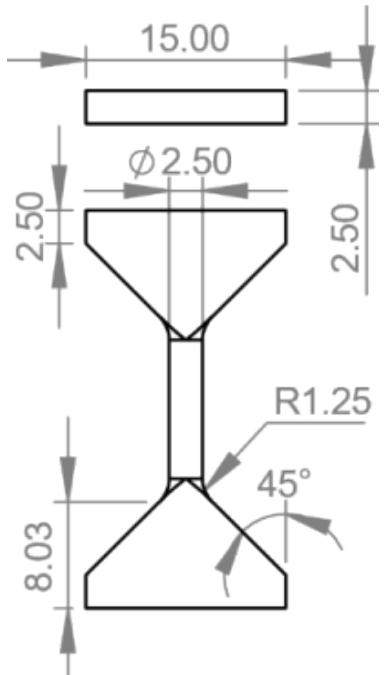
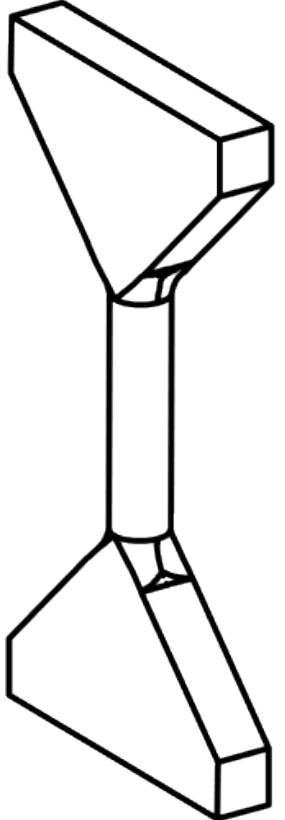
AlSi10Mg

1. What is the effect of heat treatment on mechanical properties?
2. What is the effect of porosity on mechanical properties?
3. Can we attribute failure location to specific defects?

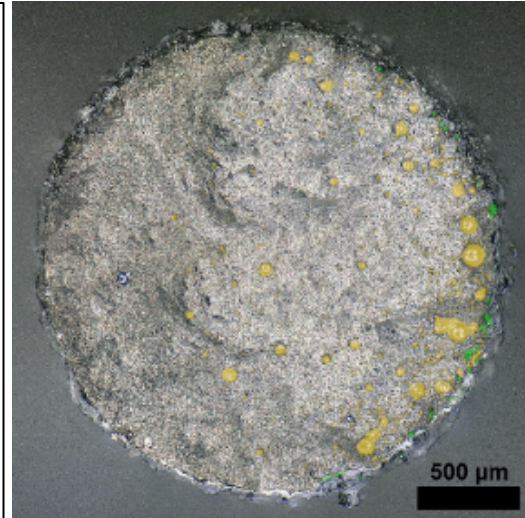
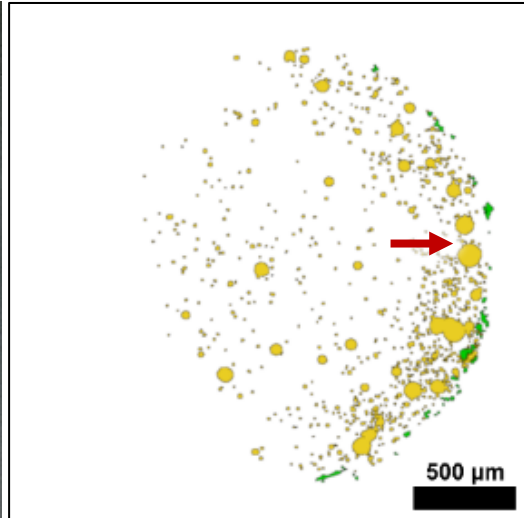
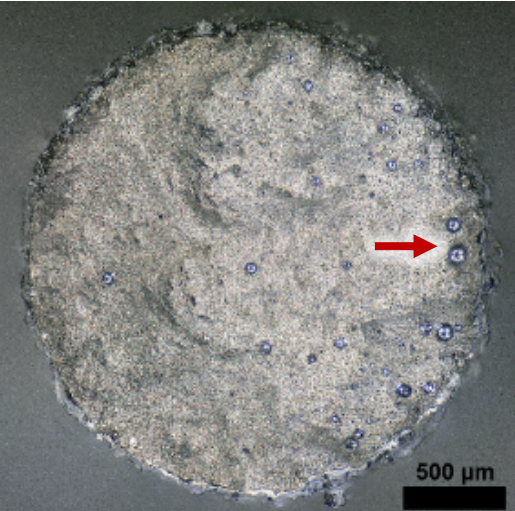


Verify pores mapped to fracture surface match fracture surface

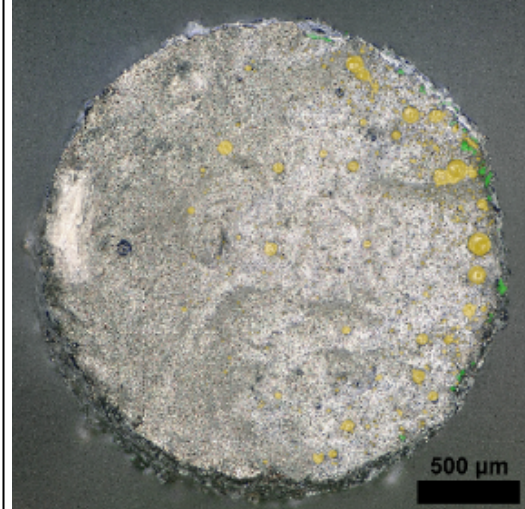
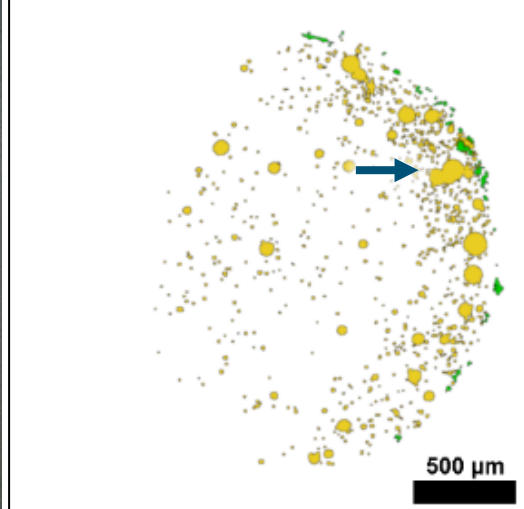
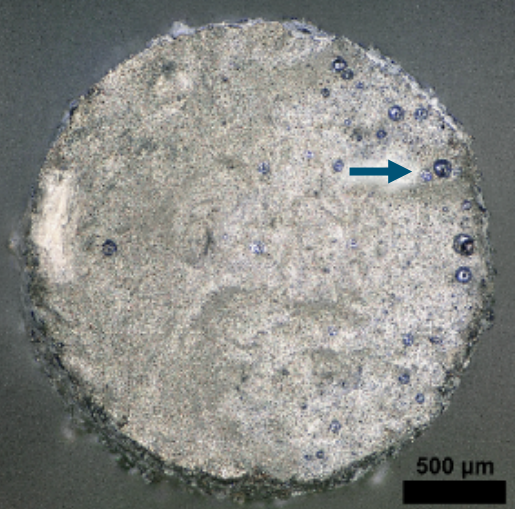
- Fracture surface is not planar.
- Pores are considered on the fracture surface if within $\pm 50 \mu\text{m}$.
- Visually verified alignment.



Top Fracture Surface

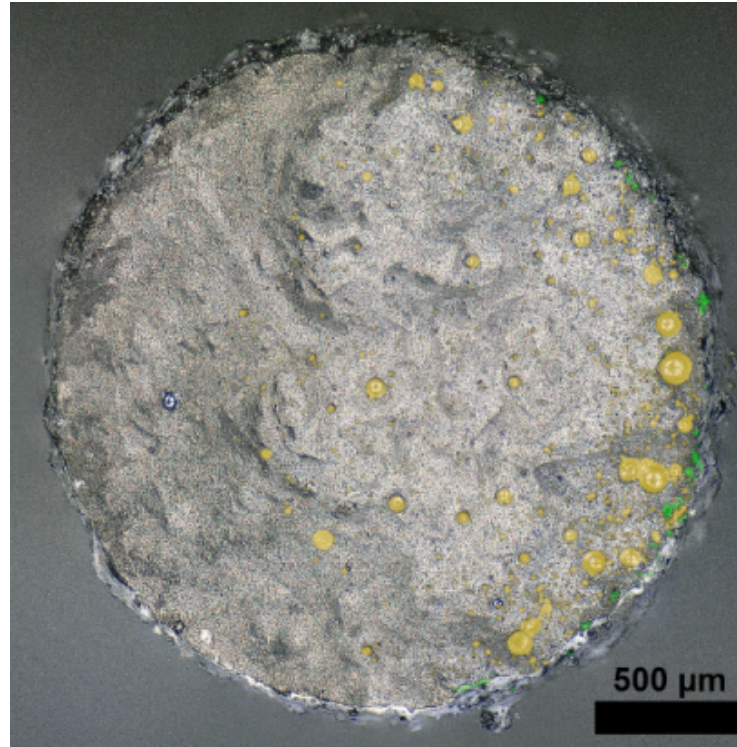
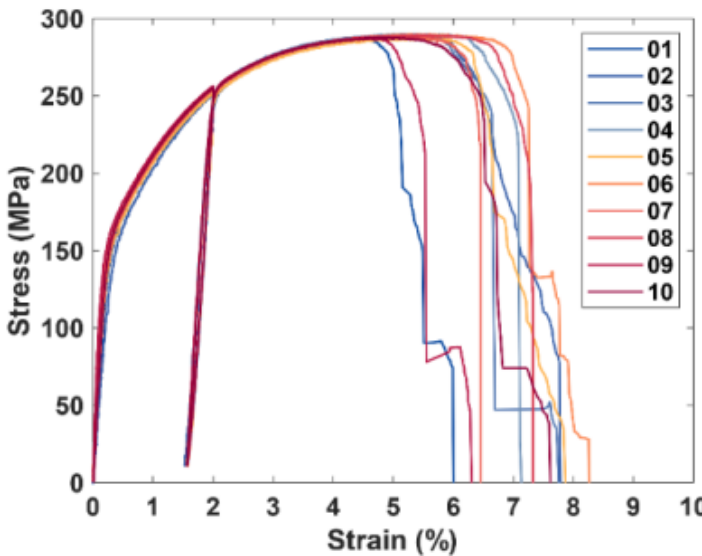


Bottom Fracture Surface

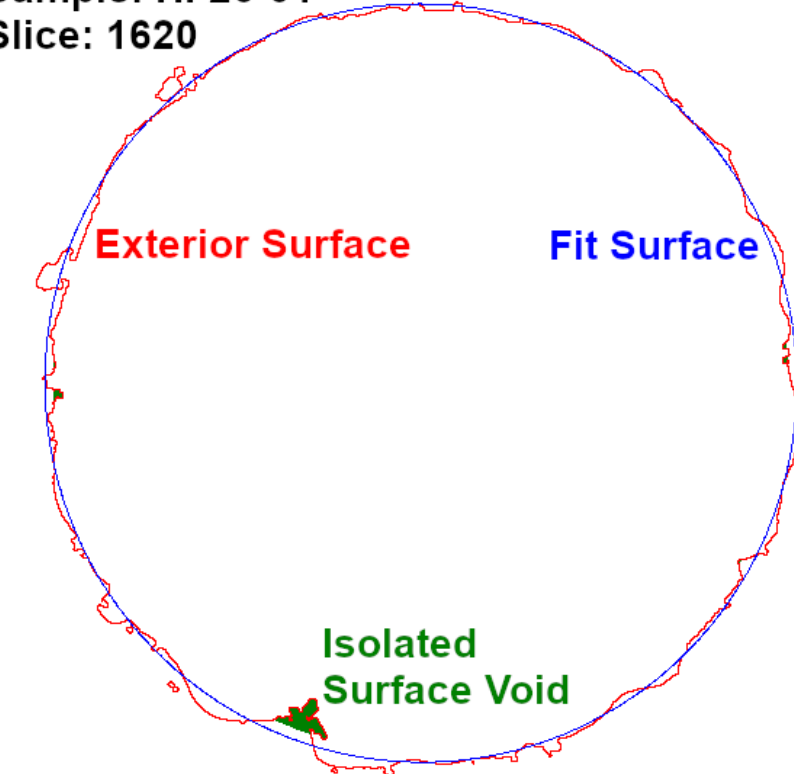


Surface flaws and internal pores are primary two features of interest.

- 10 tensile bars
- Internal pores
- Surface flaws



Sample: HF26-01
Slice: 1620

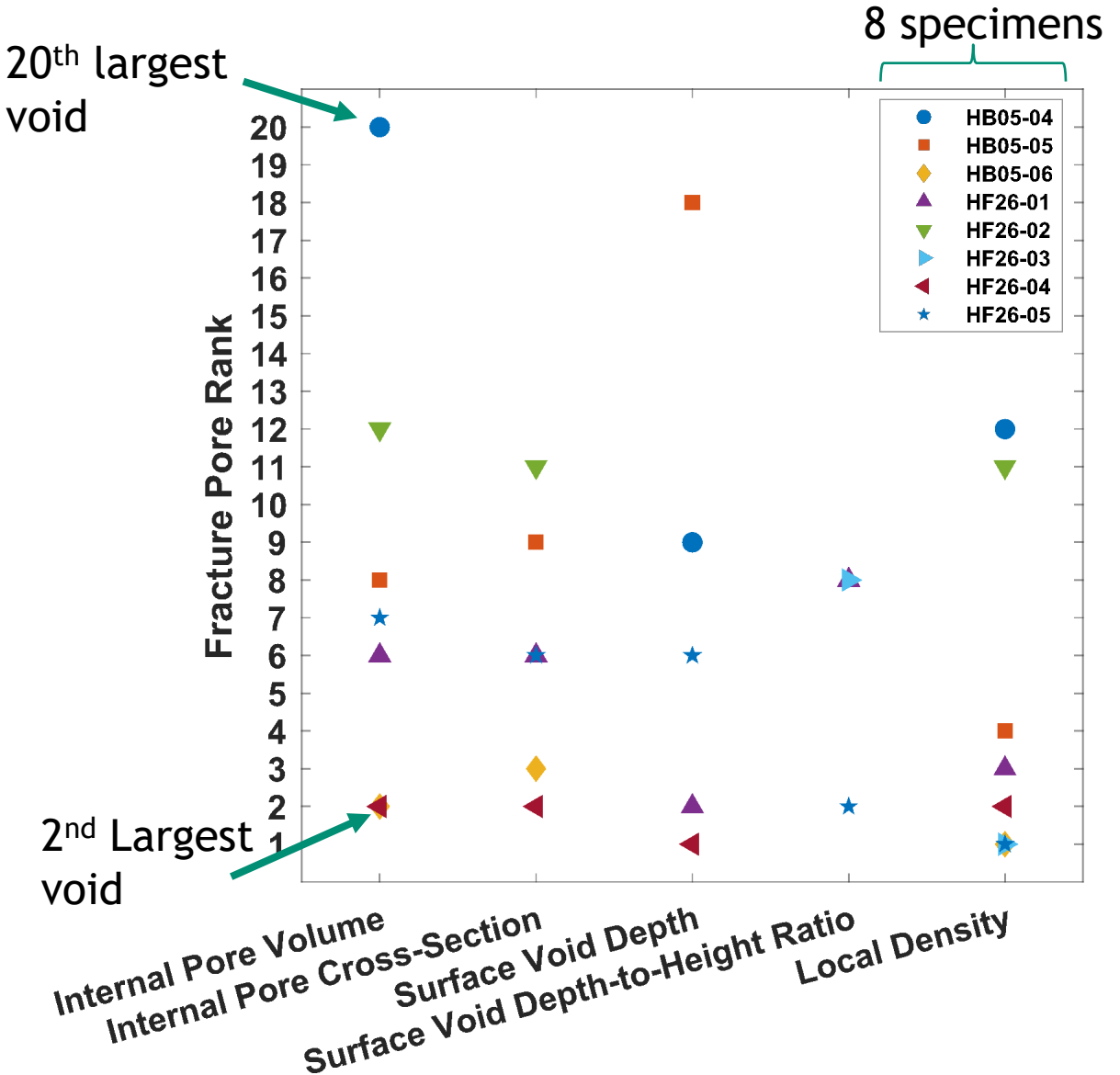


Identify dominant parameters leading to fracture by ranking.

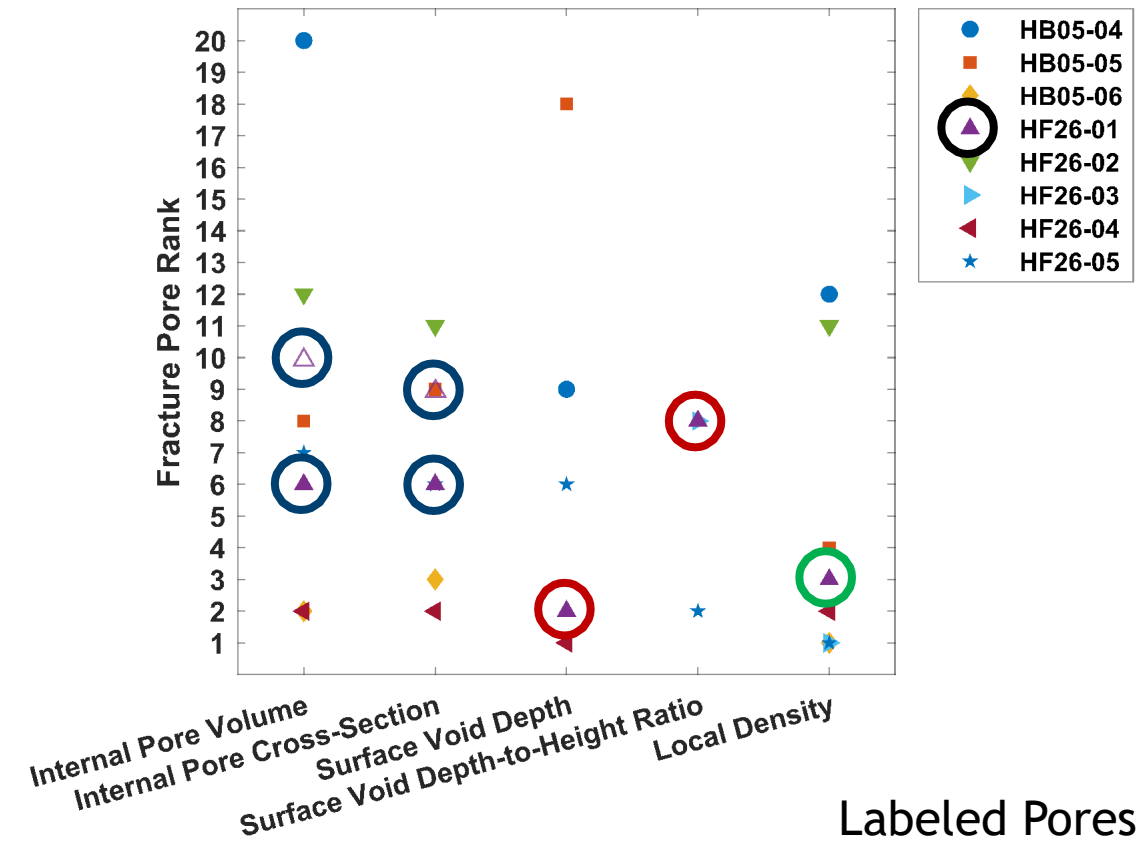
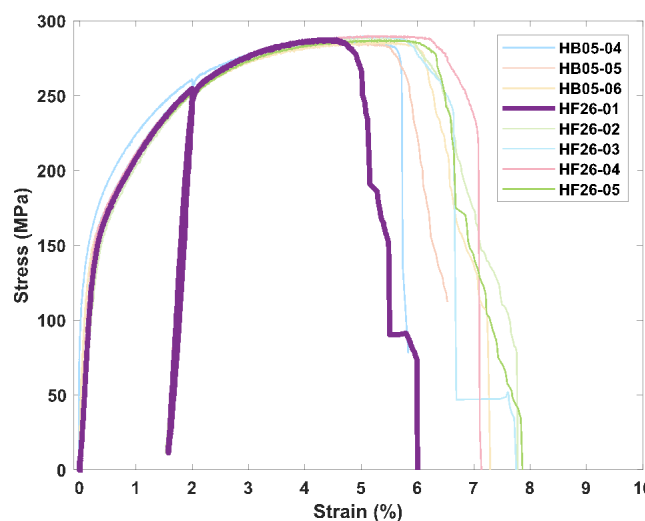
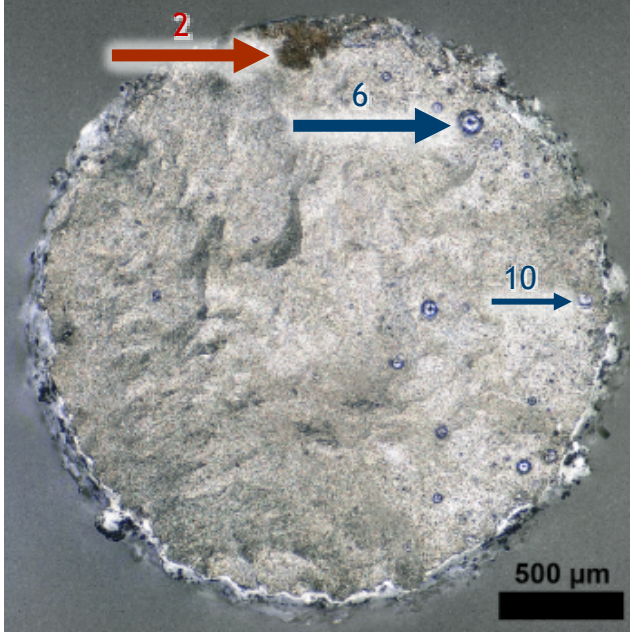
- Rank flaws on several metrics.
- Dominant parameters will have many high-ranked features on the fracture surface.

Parameters

- Largest pore volume on fracture surface
- Largest cross-sectional area of internal pores
- Deepest surface Void
- Sharpest surface void (height-to-depth ratio)
- Lowest regional density (200 μm thick slices, ~100 per specimen)

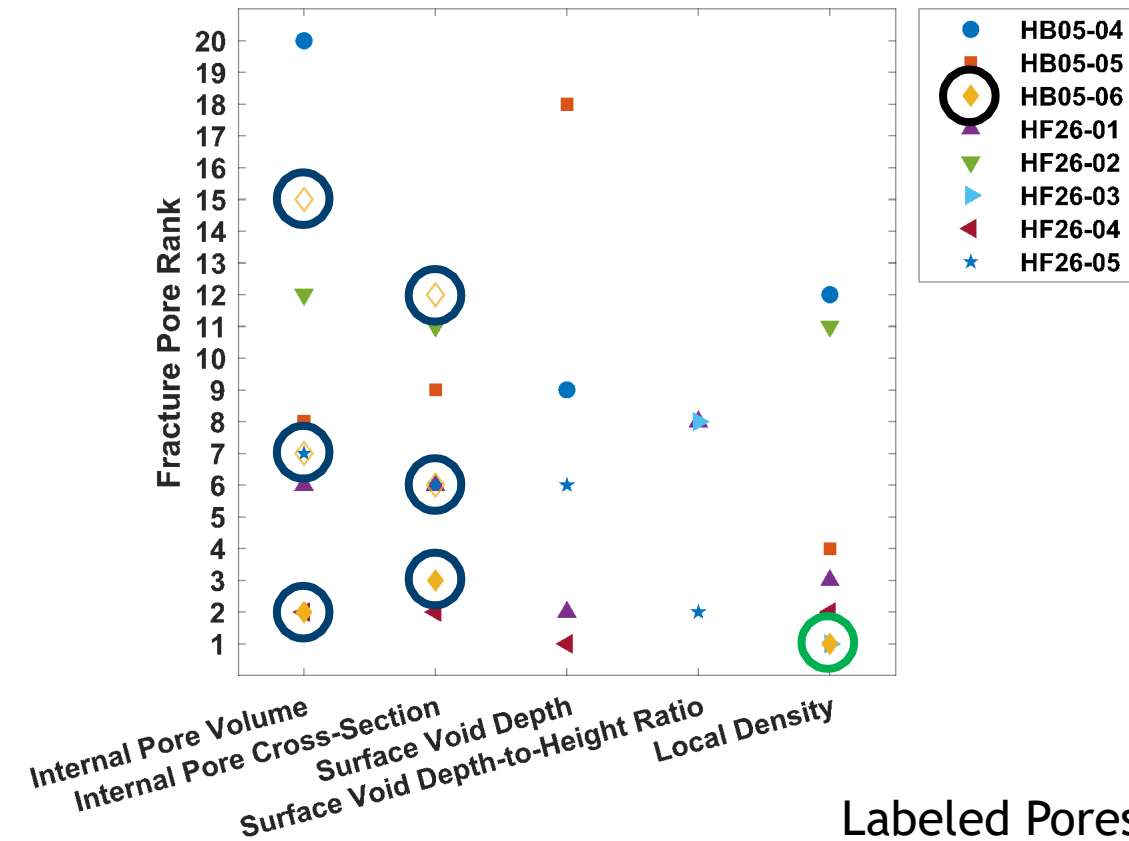
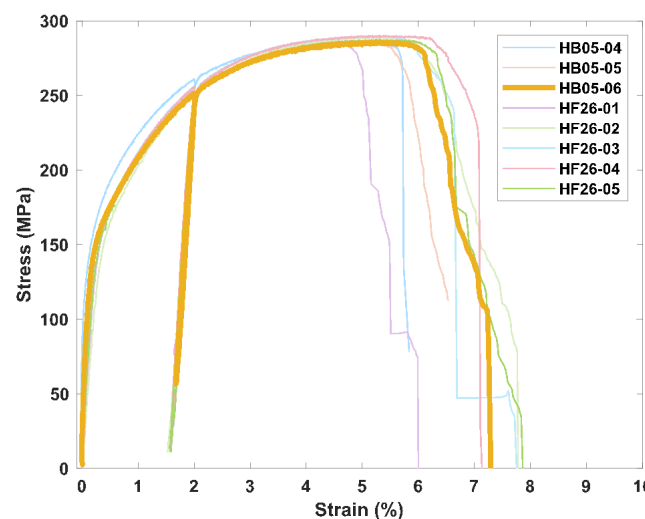
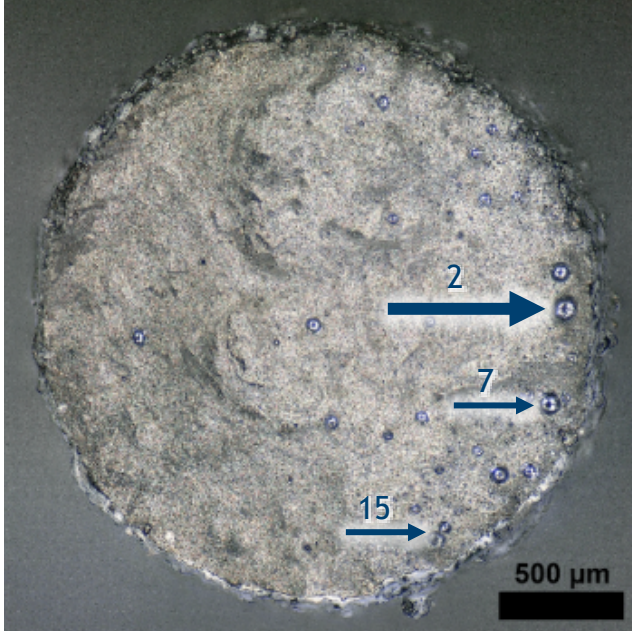


Failure of specimen HF26-01 was largely determined by surface void depth.



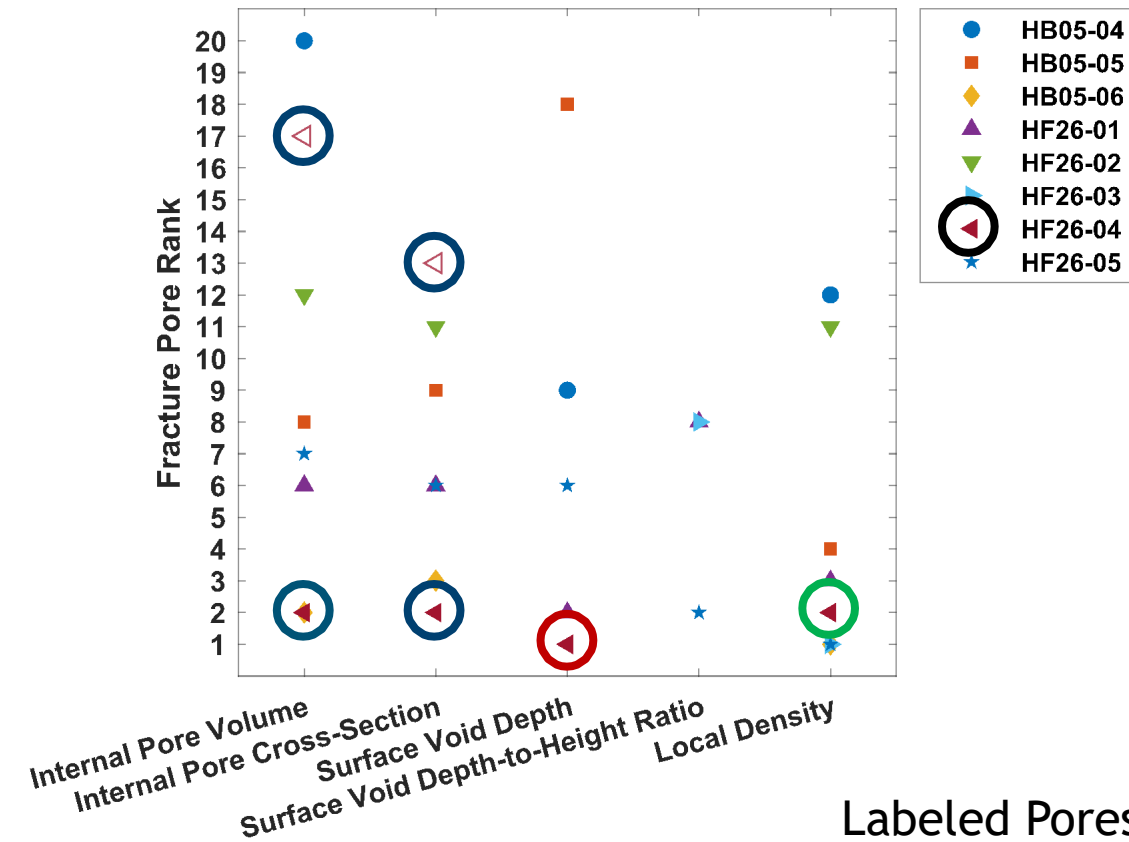
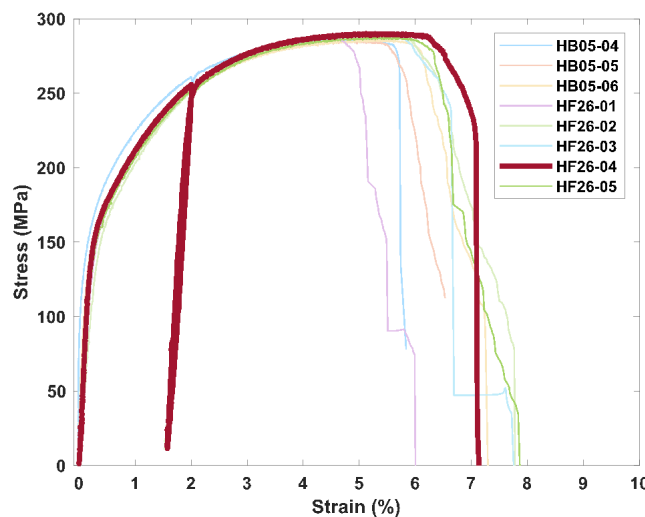
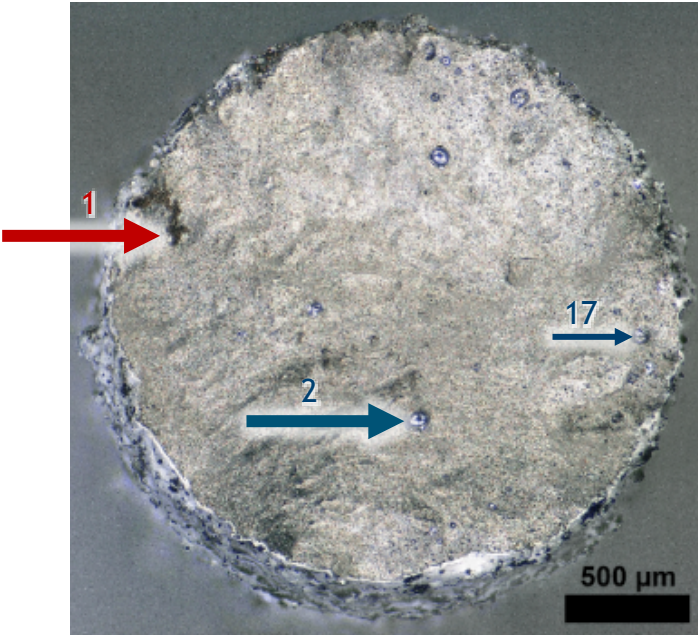
HF26-05	Internal Pore Volume	Internal Pore Cross-Section	Surface Void Depth	Surface Void Depth-to-Height	Local Density
Rank	6	6	2	8	3
Pore Label	83322	83322	83964	7520	1297
Fracture Value	730,294 μm^3	10,522 μm^2	168.8 μm	9.49	99.727 %
Peak Value	2,045,810 μm^3	24,204 μm^2	197.1 μm	16.67	99.687 %

Failure of specimen HB05-06 was largely determined by local density and several large pores.



HF26-05	Internal Pore Volume	Internal Pore Cross-Section	Surface Void Depth	Surface Void Depth-to-Height	Local Density
<i>Rank</i>	2	3	77.5	47	1
<i>Pore Label</i>	41030	41030	43203	45059	1617
<i>Fracture Value</i>	1,113,681 μm^3	12,081 μm^2	72.2 μm	9.23	99.402 %
<i>Peak Value</i>	1,447,799 μm^3	13,191 μm^2	128.0 μm	20.25	99.402 %

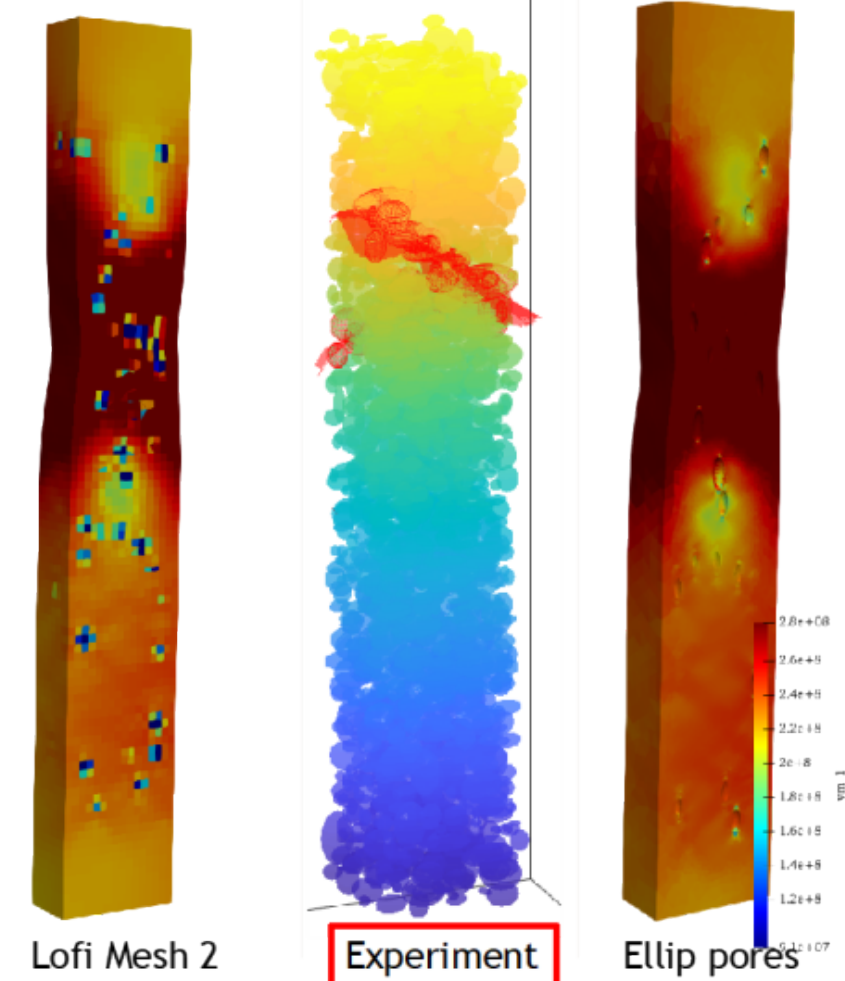
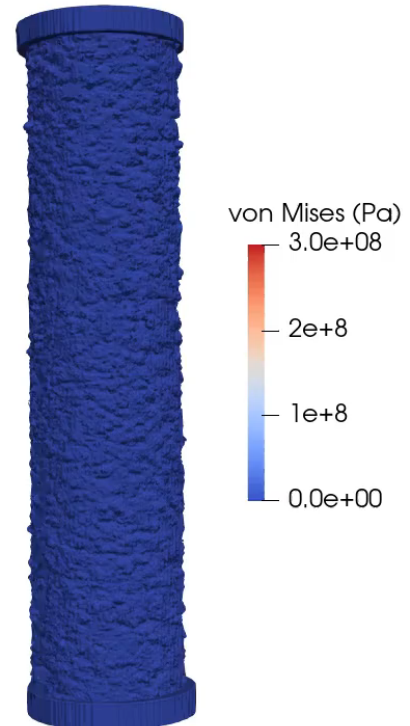
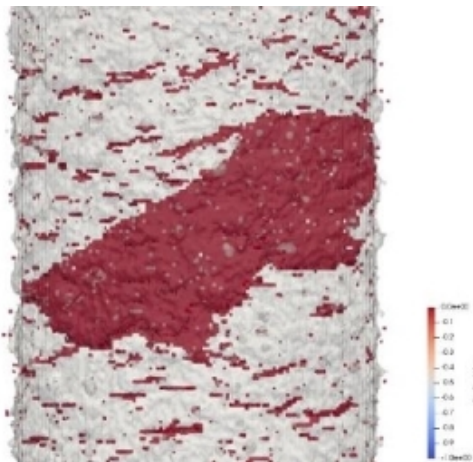
Failure of specimen HF26-04 was caused by many factors: a large surface flaw, several large internal voids, and low local density.



HF26-05	Internal Pore Volume	Internal Pore Cross-Section	Surface Void Depth	Surface Void Depth-to-Height	Local Density
Rank	2	2	1	43.5	3
Pore Label	7565	7565	9480	8040	1156
Fracture Value	580,576 μm^3	12,975 μm^2	264.4 μm	5.66	99.786 %
Peak Value	880,867 μm^3	14,514 μm^2	264.4 μm	15.68	99.783 %

Future and ongoing work

1. Hierarchical finite element model to better understand interactions between pores.
2. Machine learning on large, rich datasets to gain predictive capabilities. ([See Kyle Johnson, 3:45 Session VIII, 207A](#)).
3. Apply lessons learned to component qualification.



Courtesy of John Emery